

Phenomenology of Littlest Higgs Model with T-parity: including effects of T-odd fermions

Alexander Belyaev, Chuan-Ren Chen, Kazuhiro Tobe, C.-P. Yuan

Department of Physics and Astronomy,

Michigan State University, East Lansing, MI 48824, USA

(Dated: August 3, 2018)

We study the collider phenomenology of a Littlest Higgs model with T-parity. We first stress the important role of the T-odd $SU(2)$ doublet fermions (introduced to make the model T-parity invariant) in high energy scattering processes, such as $q\bar{q} \rightarrow W_H^+ W_H^-$ where W_H^\pm are the T-odd partners of W -bosons. Because the mass of the T-odd $SU(2)$ doublet fermions cannot be too heavy to be consistent with low energy data, they can be copiously produced at the CERN Large Hadron Collider (LHC). Therefore, we study the collider phenomenology of the model with emphasis on the contributions of the T-odd fermion to the production of the heavy T-parity partners (either bosons or fermions) of the usual particles at the LHC. The production cross sections and the decay branching ratios of the new heavy particles are classified and various experimental signatures are discussed.

I. INTRODUCTION

The standard model (SM) is an excellent low energy description of the elementary particles. The absence of any significant deviations from the SM predictions on the electroweak precision measurements suggests that the cutoff scale of the SM, as a low energy effective theory, is as large as, or larger than, 10 TeV [1]. However, having such a relatively high cutoff scale in the SM, the Higgs boson receives a large radiative correction to its mass parameter and therefore, the SM requires unsatisfactory fine-tuning to yield a correct scale of the electroweak symmetry breaking. This fine-tuning problem of the Higgs mass parameter (known as the “Little hierarchy problem”) has been one of the driving forces to consider physics beyond the SM. Moreover, a recent finding of the necessity of dark matter candidate also provides a strong motivation to seek for physics beyond the SM.

It has been shown recently that the collective symmetry breaking mechanism in the Little Higgs models [2] can provide an interesting solution to the Little hierarchy problem and the Littlest Higgs (LH) [3] model is the most economical Little Higgs model discussed in the literature. However, the original version of the LH model suffers from precision electroweak constraints [4] and the value of f , which characterizes the mass scale of new particles in the model, is forced to be larger than about 4 TeV. Since the cutoff scale of the model is about $4\pi f$, the fine tuning between the cutoff scale and the weak scale will be needed again for a too large value of f . The Littlest Higgs model with T-parity (LHT) [5, 6, 7, 8] is one of the attractive Little Higgs models. It provides a possible dark matter candidate [9] and furthermore, all dangerous tree-level contributions to low energy electroweak (EW) observables are forbidden by T-parity and hence the corrections to low energy EW observables are loop-suppressed and small. As a result, the relatively low new particle mass scale f is still allowed by data, e.g., $f > 500$ GeV [7].

The LHT predicts heavy T-odd gauge bosons which are T-parity partners of the SM gauge bosons. Moreover, in order to implement T-parity in the fermion sector, one introduces the heavy T-odd $SU(2)$ -doublet fermions, which are T-parity partners of the SM $SU(2)$ -doublet fermions and unique to Little Higgs models with T-parity. Therefore, having the relatively low new particle mass scale f , the CERN Large Hadron Collider (LHC) will have a great potential to directly produce the T-parity partners of the SM particles, and hence it is important to probe the LHT at the LHC.

In previous works on studying the phenomenology of the LHT [6], the effects of T-odd $SU(2)$ doublet fermions were not included. A preliminary study on the phenomenology of these T-odd $SU(2)$ -doublet fermions in the LHT was reported in Ref. [10]. Although, motivated by the dark matter consideration, Ref. [11] studied some interesting processes which include the effects of T-odd $SU(2)$ doublet fermions, a complete study on the phenomenology of these T-odd fermions in the LHT has not yet been presented.

In this paper, we first stress the important role of the T-odd fermions in high energy scattering processes relevant to the LHC, such as $q\bar{q} \rightarrow W_H^+ W_H^-$, where W_H^\pm is the T-parity partner of W -boson. We show that it is necessary to include the contribution from the t-channel process, via the exchange of these T-odd heavy fermions, to render its scattering amplitude with a good high energy behavior, so that its partial-wave amplitudes respect the unitarity condition. We also show that its numerical effect cannot be ignored for studying the

collider phenomenology at the LHC. Furthermore, since the current experimental constraints of the four-fermion contact interactions place an upper bound on the T-odd $SU(2)$ doublet fermion masses [7], we find not only that the T-odd fermion contribution to $q\bar{q} \rightarrow W_H^+ W_H^-$ is quantitatively important, but also that the direct pair production rate of the T-odd fermions could be significant at the LHC. To illustrate this point, we classify all production processes of the new heavy particles predicted by the LHT, and calculate the corresponding production cross sections and decay branching ratios, including the effects induced by the T-odd $SU(2)$ doublet fermions. The rest of this paper is organized as follows. In Sec. II, we briefly review the model we study here, a Littlest Higgs model with T-parity. In Sec. III, we discuss the high energy behavior of $u\bar{u} \rightarrow W_H^+ W_H^-$ process to illustrate the importance of the T-odd $SU(2)$ doublet fermion contribution to high energy scattering processes, in order to restore the unitarity of partial wave amplitudes. In Sec. IV, we show our numerical results of the phenomenological study on the Littlest Higgs model with T-parity at the LHC energy. Our conclusion is given in Sec. V.

II. A LITTLEST HIGGS MODEL WITH T-PARITY

In this section, we briefly review the Littlest Higgs Model with T-parity studied in [5, 6, 7] and present our notation of the model. The Littlest Higgs model is based on an $SU(5)/SO(5)$ non-linear sigma model [3]. A vacuum expectation value (VEV) of an $SU(5)$ symmetric tensor field (Σ_0) breaks the $SU(5)$ to $SO(5)$ at the scale f with

$$\Sigma_0 = \begin{pmatrix} 0 & 0 & 0 & 1 & 0 \\ 0 & 0 & 0 & 0 & 1 \\ 0 & 0 & 1 & 0 & 0 \\ 1 & 0 & 0 & 0 & 0 \\ 0 & 1 & 0 & 0 & 0 \end{pmatrix}. \quad (1)$$

A subgroup $[SU(2)_1 \times U(1)_1] \times [SU(2)_2 \times U(1)_2]$ of the $SU(5)$ is gauged, and at the scale f it is broken into the SM electroweak symmetry $SU(2)_L \times U(1)_Y$. The 14 Nambu-Goldstone bosons Π^a associated with the global symmetry breaking decompose under $SU(2)_L \times U(1)_Y$ as $\mathbf{1}_0 \oplus \mathbf{3}_0 \oplus \mathbf{2}_{1/2} \oplus \mathbf{3}_1$ and they are parametrized by the non-linear sigma model field $\Sigma = \xi^2 \Sigma_0$ as the fluctuations around the VEV in the broken directions, where $\xi = e^{i\Pi^a X^a/f}$ and X^a are the generators of the broken symmetry. The components $\mathbf{1}_0$ and $\mathbf{3}_0$ in the

Nambu-Goldstone boson multiplet are eaten by the heavy gauge bosons associated with the gauge symmetry breaking. The $SU(2)$ doublet $\mathbf{2}_{1/2}$ is considered to be the Higgs doublet. The doublet $\mathbf{2}_{1/2}$ and the triplet $\mathbf{3}_1$ Higgs bosons remain in the low energy effective theory, which are introduced through:

$$\Pi^a X^a = \begin{pmatrix} \mathbf{0}_{2 \times 2} & \frac{H}{\sqrt{2}} & \Phi \\ \frac{H^\dagger}{\sqrt{2}} & 0 & \frac{H^T}{\sqrt{2}} \\ \Phi^\dagger & \frac{H^*}{\sqrt{2}} & \mathbf{0}_{2 \times 2} \end{pmatrix} \text{ with } H = \begin{pmatrix} -i\pi^+ \\ \frac{h+i\pi^0}{\sqrt{2}} \end{pmatrix} \text{ and } \Phi = \begin{pmatrix} -i\phi^{++} & -i\frac{\phi^+}{\sqrt{2}} \\ -i\frac{\phi^+}{\sqrt{2}} & -i\frac{\phi^0+i\phi^P}{\sqrt{2}} \end{pmatrix}, \quad (2)$$

where $\mathbf{0}_{2 \times 2}$ is a two by two matrix with zero components and the superscript T denotes taking transpose. Here we only show the doublet Higgs $H(\mathbf{2}_{1/2})$, where π^+ and π^0 are eaten by the SM W^- and Z -bosons, respectively, and the triplet Higgs $\Phi(\mathbf{3}_1)$, which forms a symmetric tensor with components $\phi^{\pm\pm}$, ϕ^\pm , ϕ^0 and ϕ^P [12]. Since the non-linear sigma model field Σ transforms as $\Sigma \rightarrow V\Sigma V^T$ under the $SU(5)$ rotation V , its gauge-invariant kinetic term is given by

$$\mathcal{L} = \frac{f^2}{8} \text{Tr}(D_\mu \Sigma)^\dagger (D^\mu \Sigma), \quad (3)$$

where the covariant derivative D_μ for the $[SU(2)_1 \times U(1)_1] \times [SU(2)_2 \times U(1)_2]$ gauge symmetry is defined as

$$D_\mu \Sigma = \partial_\mu \Sigma - i \sum_{A=1,2} [\bar{g}_A (W_{A\mu}^a Q_A^a \Sigma + \Sigma Q_A^a W_{A\mu}^a) + \bar{g}'_A (B_{A\mu} Y_A \Sigma + \Sigma Y_A B_{A\mu})]. \quad (4)$$

Here $W_{A\mu}^a$ and $B_{A\mu}$ ($A = 1, 2$) are gauge bosons, and \bar{g}_A and \bar{g}'_A are gauge couplings for $SU(2)_A$ and $U(1)_A$ gauge symmetries, respectively. They are related to the SM gauge couplings g for $SU(2)_L$ and g' for $U(1)_Y$ as $1/g^2 = 1/\bar{g}_1^2 + 1/\bar{g}_2^2$ and $1/g'^2 = 1/\bar{g}_1'^2 + 1/\bar{g}_2'^2$. The generators for $SU(2)_A$ (denoted as Q_A^a) and for $U(1)_A$ (denoted as Y_A) are explicitly expressed as

$$Q_1^a = \begin{pmatrix} \sigma^a/2 & \mathbf{0}_2 & \mathbf{0}_{2 \times 2} \\ \mathbf{0}_2^T & 0 & \mathbf{0}_2^T \\ \mathbf{0}_{2 \times 2} & \mathbf{0}_2 & \mathbf{0}_{2 \times 2} \end{pmatrix}, \quad Q_2^a = \begin{pmatrix} \mathbf{0}_{2 \times 2} & \mathbf{0}_2 & \mathbf{0}_{2 \times 2} \\ \mathbf{0}_2^T & 0 & \mathbf{0}_2^T \\ \mathbf{0}_{2 \times 2} & \mathbf{0}_2 & -\sigma^{a*}/2 \end{pmatrix}, \quad (5)$$

$$Y_1 = \text{diag.}(3, 3, -2, -2, -2)/10, \quad Y_2 = \text{diag.}(2, 2, 2, -3, -3)/10, \quad (6)$$

where σ^a is the Pauli matrix, $\mathbf{0}_2 = (0, 0)^T$ and “diag.” denotes a diagonal matrix.

A. Gauge boson sector

T-parity [5, 8] is naturally introduced in this framework. It exchanges $[SU(2)_1 \times U(1)_1]$ and $[SU(2)_2 \times U(1)_2]$ symmetries. For example, $W_{1\mu}^a \leftrightarrow W_{2\mu}^a$ and $B_{1\mu} \leftrightarrow B_{2\mu}$ under T-parity. The Lagrangian Eq. (3) is invariant under T-parity if $\bar{g}_1 = \bar{g}_2$ and $\bar{g}'_1 = \bar{g}'_2$ and Σ transforms as $\Sigma \rightarrow \tilde{\Sigma} = \Sigma_0 \Omega \Sigma^\dagger \Omega \Sigma_0$ with $\Omega = \text{diag.}(1, 1, -1, 1, 1)$. Note that the doublet Higgs H (triplet Higgs Φ) is even (odd) under T-parity. The T-even combinations of the gauge fields are SM $SU(2)_L$ gauge bosons (W_μ^a) and $U(1)_Y$ hypercharge gauge boson (B_μ), defined as $W_\mu^a = \frac{W_{1\mu}^a + W_{2\mu}^a}{\sqrt{2}}$ and $B_\mu = \frac{B_{1\mu} + B_{2\mu}}{\sqrt{2}}$. The T-odd combinations are T-parity partners of the SM gauge bosons. After taking into account electroweak symmetry breaking, the masses of the T-parity partners of the photon (A_H), Z -boson (Z_H) and W -boson (W_H) are given by

$$M_{A_H} = \frac{g'f}{\sqrt{5}} \left[1 - \frac{5v_{SM}^2}{8f^2} + \dots \right], \quad M_{Z_H} \simeq M_{W_H} = gf \left[1 - \frac{v_{SM}^2}{8f^2} + \dots \right]. \quad (7)$$

Here v_{SM} is the electroweak breaking scale, $v_{SM} \simeq 246$ GeV, so that at tree level the SM gauge boson masses can be expressed as $M_W = \frac{g}{2}v_{SM}$ and $M_Z = \frac{\sqrt{g^2 + g'^2}}{2}v_{SM}$ for W -boson and Z -boson, respectively. Because of the smallness of g' , the T-parity partner of the photon A_H tends to be the lightest T-odd particle in this framework. Since the lightest T-odd particle is stable, it can be an interesting dark matter candidate [9].

Because of the T-parity, SM gauge bosons do not mix with the T-odd heavy gauge bosons even after the electroweak symmetry breaking. Consequently, the low energy EW observables are not modified at tree level. Since the new heavy T-odd particles always contribute to loops in pairs, the loop corrections to the EW observables are typically small. As a result, the new particle mass scale f can be as low as 500 GeV [7], and hence, T-odd heavy gauge bosons can be copiously produced at the LHC.

B. T-odd $SU(2)$ doublet fermion sector

To implement T-parity in the fermion sector, one introduces two $SU(2)$ fermion doublets q_i ($i = 1, 2$) for each SM fermion doublet [5, 6, 7]. Here q_i are the doublet under $SU(2)_i$ ($i = 1, 2$), and T-parity exchanges q_1 and q_2 . The T-even combination of q_i is the SM fermion doublet and the other T-odd combination is its T-parity partner. To generate a heavy mass for the T-odd fermion doublet, we introduce the following interaction, as

suggested in Ref. [5, 6, 7]:

$$\mathcal{L}_\kappa = -\kappa f(\bar{\Psi}_2 \xi \Psi_c + \bar{\Psi}_1 \Sigma_0 \Omega \xi^\dagger \Omega \Psi_c) + \text{hermitian conjugate (h.c.)}. \quad (8)$$

Here the fermion $SU(2)$ doublets q_1 and q_2 are embedded into incomplete $SU(5)$ multiplets Ψ_1 and Ψ_2 as $\Psi_1 = (q_1, 0, \mathbf{0}_2)^T$ and $\Psi_2 = (\mathbf{0}_2, 0, q_2)^T$, and the doublets q_1 and q_2 are explicitly written as $q_A = -\sigma_2 (u_{LA}, d_{LA})^T = (id_{LA}, -iu_{LA})^T$ with $A = 1, 2$. Under the global $SU(5)$, the multiplets Ψ_1 and Ψ_2 transform as $\Psi_1 \rightarrow V^* \Psi_1$ and $\Psi_2 \rightarrow V \Psi_2$, where V is an $SU(5)$ rotation matrix. A multiplet Ψ_c is also introduced as $\Psi_c = (q_c, \chi_c, \tilde{q}_c)^T$, which transforms non-linearly under $SU(5)$: $\Psi_c \rightarrow U \Psi_c$ where U is an unbroken $SO(5)$ rotation matrix in non-linear representation of $SU(5)$. The object ξ and the non-linear sigma model field $\Sigma (\equiv \xi^2 \Sigma_0)$ transform like $\xi \rightarrow V \xi U^\dagger = U \xi \Sigma_0 V^T \Sigma_0$ and $\Sigma \rightarrow V \Sigma V^T$, respectively, under $SU(5)$. T-parity transformation laws are defined as follows: $\Psi_1 \leftrightarrow -\Sigma_0 \Psi_2$, $\Psi_c \rightarrow -\Psi_c$, and $\xi \rightarrow \Omega \xi^\dagger \Omega$. Thus, $q_1 \leftrightarrow -q_2$ and $\Sigma \rightarrow \tilde{\Sigma} \equiv \Sigma_0 \Omega \Sigma^\dagger \Omega \Sigma_0$ under T-parity. One can verify that the interaction in Eq. (8) is invariant under T-parity.

From the interaction in Eq. (8), one can see that the T-odd fermion doublet $q_- \equiv (q_1 + q_2)/\sqrt{2} = (id_{L-}, -iu_{L-})^T$ gets a Dirac mass, with $\tilde{q}_c \equiv (id_{R-}, -iu_{R-})^T$, as

$$M_{d-} \simeq \sqrt{2} \kappa f, \quad M_{u-} \simeq \sqrt{2} \kappa f \left(1 - \frac{v_{SM}^2}{8f^2} + \dots \right). \quad (9)$$

One may think that assuming a large κ value, these T-odd fermions will decouple and hence we may ignore any effects induced by the T-odd $SU(2)$ doublet fermions. However, as pointed out in Ref. [7], there is non-decoupling effect in some four-fermion operators whose coefficients become larger as the magnitude of κ increases. The constraint on the four-fermion contact interaction contributing to the $e^+ e^- \rightarrow q \bar{q}$ scattering sets an important upper bound on the T-odd fermion masses M_{q-} as [7]

$$M_{q-} < 4.8 \left(\frac{f}{1 \text{ TeV}} \right)^2 \text{ TeV}. \quad (10)$$

Here we have assumed a universal κ value to all T-odd fermion couplings generated by Eq. (8). Therefore, the effect of T-odd fermions to high energy collider phenomenology may not be negligible, and actually it is quantitatively important as we will discuss in later sections. The interaction terms in Eq. (8) in general contain flavor indices, and large flavor mixings can cause flavor-changing-neutral-current (FCNC) problem [13]. For simplicity, we assume the flavor diagonal and universal κ in this study.

	q_1	q_2	U_{L_1}	U_{L_2}	U_{R_1}	U_{R_2}	u_{R_+}	d_{R_+}
Y_1	1/30	2/15	8/15	2/15	8/15	2/15	1/3	-1/6
Y_2	2/15	1/30	2/15	8/15	2/15	8/15	1/3	-1/6

TABLE I: $U(1)_A$ charges Y_A for fermions. The SM hypercharge is given by $Y = Y_1 + Y_2$.

In the multiplet Ψ_c , there are other extra T-odd fermions. For those fermions, we simply assume Dirac masses, as suggested in Ref. [5, 8]. Furthermore, we assume that their Dirac masses are so large (as large as about 3 TeV) that these extra T-odd fermions are decoupled, but remains to be small enough not to generate the naturalness problem in the Higgs mass parameter. Thus, in our following analysis, we will not consider any effects induced by these extra T-odd fermions.

The $U(1)_A$ charges Y_A for fermions are listed in Table I.¹ Those charges are determined by the gauge invariance of the Yukawa couplings which we will discuss later. In addition to the normal SM gauge interactions, the T-odd fermions interact with their SM partner fermions and the heavy gauge boson as follows:

$$\begin{aligned} \mathcal{L} = & \frac{g}{\sqrt{2}} W_{H\mu}^+ (\bar{u}_L \gamma_\mu d_{L-} + \bar{u}_{L-} \gamma_\mu d_L) + \text{h.c.} \\ & + \sum_{f=u,d} [(gc_H T_{3f} + g' s_H Y') Z_{H\mu} + (-gs_H T_{3f} + g' c_H Y') A_{H\mu}] \bar{f}_L \gamma_\mu f_{L-} + \text{h.c.}, \end{aligned} \quad (11)$$

where $Y' = -1/10$, and $s_H (\equiv \sin \theta_H)$ describes the degree of mixing between heavy neutral gauge bosons with $s_H \simeq \frac{gg'}{g^2 - g'^2/5} \frac{v_{SM}^2}{4f^2}$ and $c_H \equiv \cos \theta_H$. For clarity, the corresponding Feynman rules are presented in Appendix A. Through these interactions, the T-odd fermion can contribute to heavy gauge boson productions. Also, it can be directly produced via exchanging light gauge bosons, heavy gauge bosons, and gluons at high energy hadron colliders, such as the LHC, as we will discuss in the following sections.

C. Yukawa couplings for Top and other fermions

In order to cancel the large radiative correction to Higgs mass parameter induced by top-quark, we introduce in the top sector the singlet fields U_{L_1} and U_{L_2} , which are embedded,

¹ Strictly speaking, these $U(1)_A$ charges Y_A ($A = 1, 2$) for fermions are defined by a sum of the $U(1)_A$ charges from the original $SU(5)$ and extra fermion $U(1)$ charges.

together with the q_1 and q_2 doublets, into the following multiplets: $Q_1 = (q_1, U_{L_1}, 0_2)^T$ and $Q_2 = (0_2, U_{L_2}, q_2)^T$. For the top-Yukawa interaction, one can write down the following T-parity invariant Lagrangian: [5, 6, 7]:

$$\begin{aligned} \mathcal{L}_t = & -\frac{\lambda_1 f}{2\sqrt{2}} \epsilon_{ijk} \epsilon_{xy} \left[(\bar{Q}_1)_i \Sigma_{jx} \Sigma_{ky} - (\bar{Q}_2 \Sigma_0)_i \tilde{\Sigma}_{jx} \tilde{\Sigma}_{ky} \right] u_{R_+} \\ & - \lambda_2 f (\bar{U}_{L_1} U_{R_1} + \bar{U}_{L_2} U_{R_2}) + \text{h.c.}, \end{aligned} \quad (12)$$

where ϵ_{ijk} and ϵ_{xy} are antisymmetric tensors, and i, j and k run over 1–3 and x and y over 4–5. u_{R_+} and U_{R_i} ($i = 1, 2$) are $SU(2)$ singlets. Under T-parity, these fields transform as $Q_1 \leftrightarrow -\Sigma_0 Q_2$, $U_{R_1} \leftrightarrow -U_{R_2}$ and $u_{R_+} \rightarrow u_{R_+}$. The above Lagrangian contains the following mass terms:

$$\begin{aligned} \mathcal{L}_t \simeq & -\lambda_1 f \left[\frac{v_{SM}}{f} \left(1 - \frac{v_{SM}^2}{4f^2} + \dots \right) \bar{u}_{L_+} u_{R_+} + \left(1 - \frac{v_{SM}^2}{2f^2} \right) \bar{U}_{L_+} u_{R_+} \right] \\ & - \lambda_2 f (\bar{U}_{L_+} U_{R_+} + \bar{U}_{L_-} U_{R_-}) + \text{h.c.} \end{aligned} \quad (13)$$

Here we have defined the T-parity eigenstates as $q_+ \equiv (q_1 - q_2)/\sqrt{2} = (id_{L_+}, -iu_{L_+})$, $U_{L_\pm} = \frac{U_1 \mp U_2}{\sqrt{2}}$ and $U_{R_\pm} = \frac{U_{R_1} \mp U_{R_2}}{\sqrt{2}}$. One T-odd Dirac fermion T_- ($T_{-L} \equiv U_{L_-}$, $T_{-R} \equiv U_{R_-}$) gets a mass $M_{T_-} = \lambda_2 f$ (cf. Eq. (13)), and a T-odd combination of the doublets q_1 and q_2 obtains a mass from \mathcal{L}_κ (cf. Eq. (8)). The left-handed (or right-handed) top quark (t) is a linear combination of u_{L_+} and U_{L_+} (or u_{R_+} and U_{R_+}), and another independent linear combination is a heavy T-even partner of the top quark (T_+):

$$\begin{pmatrix} u_{X_+} \\ U_{X_+} \end{pmatrix} = \begin{pmatrix} c_X & s_X \\ -s_X & c_X \end{pmatrix} \begin{pmatrix} t_X \\ T_{+X} \end{pmatrix}, \quad (X = L, R), \quad (14)$$

where the mixings are approximately expressed by

$$s_L = s_\alpha^2 \frac{v_{SM}}{f} + \dots, \quad s_R = s_\alpha \left[1 - \frac{c_\alpha^2 (c_\alpha^2 - s_\alpha^2) v_{SM}^2}{2 f^2} + \dots \right], \quad (15)$$

with $s_\alpha = \lambda_1 / \sqrt{\lambda_1^2 + \lambda_2^2}$ and $c_\alpha = \lambda_2 / \sqrt{\lambda_1^2 + \lambda_2^2}$. The masses of the top quark (t) and T-even heavy top quark (T_+) are given by

$$M_t = \lambda_1 c_\alpha v_{SM} \left[1 - \frac{c_\alpha^4 + s_\alpha^4}{4} \frac{v_{SM}^2}{f^2} + \dots \right], \quad M_{T_+} = \frac{\lambda_1}{s_\alpha} f \left[1 - \frac{c_\alpha^2 s_\alpha^2}{2} \frac{v_{SM}^2}{f^2} + \dots \right]. \quad (16)$$

Note that the T-even heavy top (T_+) is always heavier than the T-odd heavy top (T_-) in the effective theory considered here. The Feynman rules of SM and heavy gauge boson interactions in the top sector are also summarized in Appendix A. We note that the coupling

strength of $W^+\bar{t}b$ is $V_{tb}^{eff} = V_{tb}c_L$ (see Appendix A) where V_{tb} is the (t, b) element of the Cabibbo-Kobayashi-Maskawa (CKM) matrix. For our numerical results shown below, we have assumed $V_{tb} = 1$, so that $V_{tb}^{eff} = c_L = \sqrt{1 - s_L^2}$, where s_L is given in Eq. (15). Once the V_{tb}^{eff} is measured experimentally, then the parameter space of the model can be further constrained. In other word, when the parameter s_α varies, the effective coupling strength of $W^+\bar{t}b$ also varies under our assumption $V_{tb} = 1$, so that the single-top production rate at the Tevatron and the LHC also varies. As $s_\alpha \rightarrow 0$, it is approaching to the SM $W^+\bar{t}b$ coupling strength.

In the top sector, there are two free parameters λ_1 and λ_2 , which can be replaced by λ_1 and s_α as two independent parameters. The experimental value of the top quark mass (M_t) gives the relation between λ_1 and s_α as

$$\lambda_1 = \frac{M_t}{v_{SM}} \frac{1}{\sqrt{1 - s_\alpha^2}} \geq 0.71 \quad (17)$$

for $s_\alpha \geq 0$ and $M_t = 175$ GeV. Moreover, following the method presented in Ref. [14], we calculated the $J = 1$ partial wave amplitudes in the coupled system of $(t\bar{t}, T_+\bar{T}_+, b\bar{b}, WW, Zh)$ states, which are relevant to the top Yukawa coupling, to estimate the unitarity limit of the corresponding scattering amplitudes. From the unitarity limit, we can get a mild constraint on the parameters: $s_\alpha/c_\alpha \leq 3.3$, which corresponds to

$$s_\alpha \leq 0.96 \quad \text{and} \quad \lambda_1 \leq 2.5, \quad (18)$$

cf. Eq. (17). Its detailed discussion is presented in Appendix B for completeness. We could also discuss the “naturalness” constraint on these parameters. If we calculate the one-loop contribution to the Higgs mass parameter (m_h) induced by the top sector, the correction is described by $\Delta m_h^2 = c \frac{y_t^2}{16\pi^2} M_{T_+}^2 \equiv a_H M_H^2$, where $y_t = \sqrt{2}M_t/v_{SM}$ and c is a constant of $O(1)$. This correction should not be much larger than the Higgs boson (on-shell) mass squared M_H^2 , otherwise fine-tuning is needed. Thus the coefficient a_H is a measure of the “naturalness” of the Higgs mass correction. If we take $\bar{a}_H (= a_H/2c)$ to be smaller than 10, we get the upper limit on M_{T_+} as

$$M_{T_+} \leq 6.7 \text{ TeV} \sqrt{\frac{\bar{a}_H}{10}} \left(\frac{M_H}{120 \text{ GeV}} \right). \quad (19)$$

In other word,

$$s_\alpha \geq 0.11 \sqrt{\frac{10}{\bar{a}_H}} \left(\frac{120 \text{ GeV}}{M_H} \right) \left(\frac{f}{1 \text{ TeV}} \right). \quad (20)$$

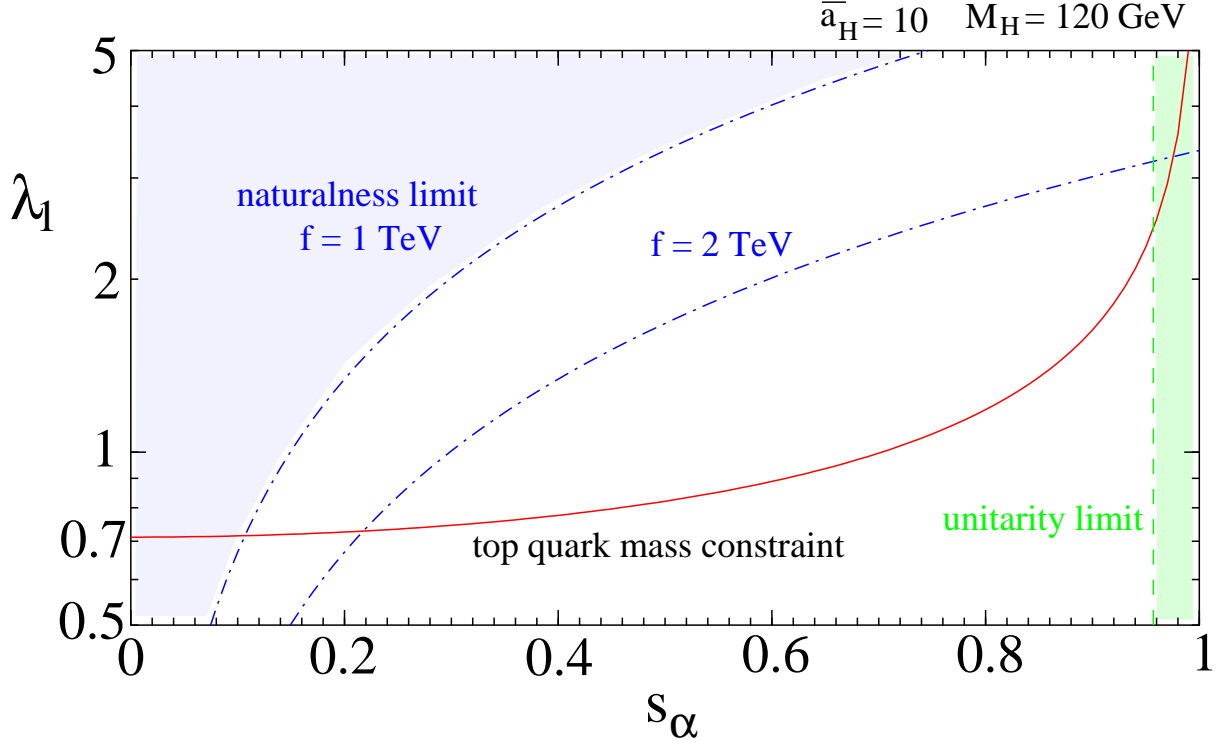


FIG. 1: Allowed region of parameters λ_1 and s_α . Solid line (red) represents a relation between λ_1 and s_α required by top quark mass ($M_t = 175$ GeV), cf. Eq. (17). Dashed line (green) shows an upper limit on s_α from the unitarity bound on the $J = 1$ partial wave amplitude in the coupled system of $(t\bar{t}, T_+\bar{T}_+, b\bar{b}, WW, Zh)$ states, as expressed in Eq. (18). Dash-dotted lines (blue) show that naturalness consideration puts lower limit on s_α (or equivalently lower limit on λ_1), as shown in Eq. (20), and the shaded region in upper-left area of the figure is excluded for $f = 1$ TeV. For $f = 2$ TeV, the excluded region is extended to the dash-dotted line with $f = 2$ TeV. Here we have assumed $\bar{a}_H = 10$ and $M_H = 120$ GeV.

We summarize these constraints on the parameters of the top sector in Fig. 1.

For the first and second generation up-type quark Yukawa couplings, we assume the same forms of Yukawa couplings as those for the top quark, cf. Eq. (13), except that we do not introduce $SU(2)$ -singlet fields U_{LA} and U_{RA} for the first and second generations because we do not require the cancellation of the quadratic divergences induced from the light quark sectors, for their Yukawa couplings are tiny.

For down-type quark Yukawa couplings, one of the possible effective Lagrangians [15, 16]² is given by

$$\mathcal{L}_{\text{down}} = \frac{i\lambda_d}{2\sqrt{2}} f \epsilon_{ij} \epsilon_{xyz} \left[(\bar{\Psi}'_2)_x \Sigma_{iy} \Sigma_{jz} X - (\bar{\Psi}'_1 \Sigma_0)_x \tilde{\Sigma}_{iy} \tilde{\Sigma}_{jz} \tilde{X} \right] d_{R+}, \quad (21)$$

where $\Psi'_1 = (-\sigma_2 q_1, 0, 0_2)^T$ and $\Psi'_2 = (0_2, 0, -\sigma_2 q_2)^T$. Here X transforms into \tilde{X} under T-parity, and it is a singlet under $SU(2)_i$ ($i = 1-2$) with its $U(1)_i$ ($i = 1-2$) charges being $(Y_1, Y_2) = (1/10, -1/10)$. In this paper, we take $X = (\Sigma_{33})^{-1/4}$, where Σ_{33} is the $(3, 3)$ component of the non-linear sigma model field Σ .

For charged lepton (neutrino) sector, we assume the same Yukawa structure as that for down-type quark (first and second generation up-type quark) sector.

D. Higgs boson sector

As we have shown, there are $SU(2)_L$ doublet and triplet Higgs bosons in the low energy effective theory. The gauge and Yukawa interactions break the global symmetry, so these Higgs bosons receive masses from radiative corrections via gauge and Yukawa interactions. Because of the collective symmetry breaking mechanism, the doublet Higgs boson does not receive large quadratic divergence in its mass parameter, and hence the natural mass scale of the doublet Higgs boson is of the order of weak scale. On the other hand, the triplet Higgs boson mass is not protected by such a mechanism, therefore, its mass scale is naturally of the order of f . Calculating the dominant quadratically divergent top- and gauge-loop corrections to the effective Higgs potential, one gets [3]

$$\begin{aligned} \mathcal{L}_{eff} = & a_t \lambda_1^2 f^4 \epsilon^{wx} \epsilon_{yz} \epsilon^{ijk} \epsilon_{klm} \left(\Sigma_{iw} \Sigma_{jx} \Sigma^{*my} \Sigma^{*lz} + \tilde{\Sigma}_{iw} \tilde{\Sigma}_{jx} \tilde{\Sigma}^{*my} \tilde{\Sigma}^{*lz} \right) \\ & + a_g f^4 \left(g^2 \text{Tr} \sum_{A=1,2} (Q_A^a \Sigma) (Q_A^a \Sigma)^* + g'^2 \text{Tr} \sum_{A=1,2} (Y_A \Sigma) (Y_A \Sigma)^* \right), \end{aligned} \quad (22)$$

$$\simeq -M_\Phi^2 \left(\text{Tr} \Phi^\dagger \Phi + \frac{h^4}{16f^2} \right) + \dots, \quad (23)$$

where a_t and a_g are constants of the order of 1. Note that because of the collective symmetry breaking mechanism, the doublet Higgs boson does not receive quadratically divergent

² We thank J. Hubisz for pointing out this possibility. The effective Lagrangian for the down-type quark Yukawa couplings proposed in Ref. [6] is not invariant under $U(1)_A$ ($A = 1, 2$).

	A_H	Z_H (W_H)	T_+	T_-	u_-	d_-	Φ
Mass (TeV)	0.15	0.65	1.4	1.0	1.4	1.4	0.69

TABLE II: Typical values of masses for the heavy T-parity partners of the SM particles. Here we take the scale f to be 1 TeV, $s_\alpha = 1/\sqrt{2}$, $\kappa = 1$, and the top quark and Higgs boson masses to be 175 and 120 GeV, respectively.

top- and gauge-loop corrections at one-loop level, however, it receives the logarithmically divergent one-loop and quadratically divergent two-loop corrections, even though we don't show them explicitly in Eq. (23). As shown in Eq. (23), the coefficient of the $\text{Tr}\Phi^\dagger\Phi$ term is $-M_\Phi^2$. Hence, the mass of the triplet Higgs boson is related to the quartic coupling of the doublet Higgs boson. Consequently, there is a relation between the triplet and doublet Higgs boson masses, which is approximately expressed as

$$M_\Phi \simeq \frac{\sqrt{2}M_H}{v_{SM}}f. \quad (24)$$

In our analysis, we take the doublet Higgs boson mass M_H as a free parameter, and we calculate the triplet Higgs boson mass using Eq. (24)³. Since the triplet Higgs multiplet can participate in electroweak interactions and the triplet Higgs boson masses can be of the order of TeV, they can be directly produced at the LHC.

In Table II, we list the typical mass spectrum of the heavy T-parity partners of the SM particles. Here we have taken the scale f to be 1 TeV, $s_\alpha = 1/\sqrt{2}$ (or, equivalently, $\lambda_1 = \lambda_2 \sim \frac{\sqrt{2}M_t}{v_{SM}} \sim 1$), $\kappa = 1$, and the top quark and Higgs boson masses to be 175 and 120 GeV, respectively. We will assume this set of model parameter values in the rest of this paper, unless otherwise stated.

III. HIGH ENERGY BEHAVIOR OF $u\bar{u} \rightarrow W_H^+W_H^-$

Before we present a detailed study on the collider phenomenology of the Littlest Higgs model with T-parity, we stress in this section the importance of the T-odd $SU(2)$ doublet

³ After the electroweak symmetry breaking, each component of the triplet Higgs multiplet receives different correction to their masses, and hence non-degeneracy will be induced. In our analysis, we have not included this non-degeneracy in the triplet mass spectrum.

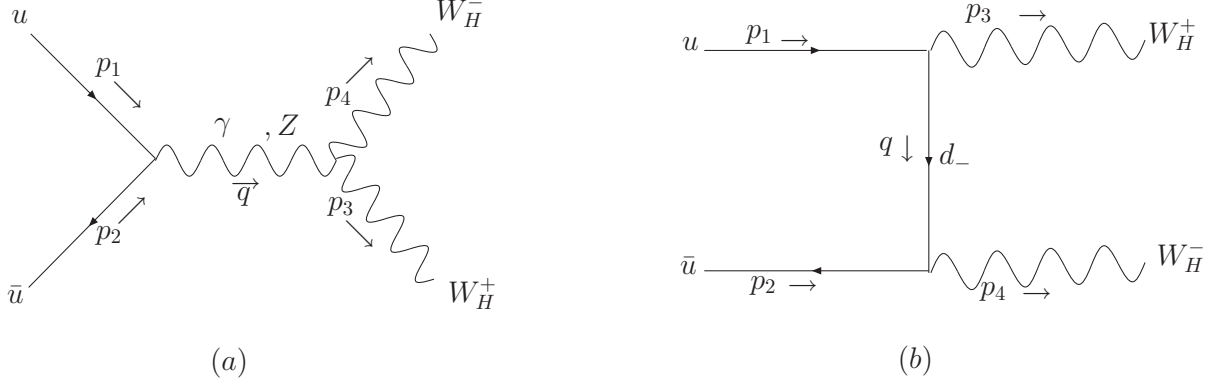


FIG. 2: Feynman diagrams for $u\bar{u} \rightarrow W_H^+ W_H^-$.

fermion contributions to high energy processes. To illustrate the important role of the T-odd $SU(2)$ doublet fermions in high energy processes, we discuss the high energy behavior of $u\bar{u} \rightarrow W_H^+ W_H^-$. The tree-level diagrams for this process are given in Fig. 2. The amplitudes of the s-channel process with photon and Z -boson exchanged are expressed by A^γ and A^Z , respectively, and the amplitude of the t-channel process with T-odd down-quark d_- exchanged is A^{d_-} . For the scattering process $u(p_1)\bar{u}(p_2) \rightarrow W_H^+(p_3)W_H^-(p_4)$, we find

$$\begin{aligned}
 A^\gamma &= \frac{2e^2}{3s} \bar{v}(p_2) \{ (-\not{p}_3 + \not{p}_4) \varepsilon^*(p_3) \cdot \varepsilon^*(p_4) \\
 &\quad - 2p_4 \cdot \varepsilon^*(p_3) \not{\varepsilon}^*(p_4) + 2p_3 \cdot \varepsilon^*(p_4) \not{\varepsilon}^*(p_3) \} u(p_1), \\
 A^Z &= \frac{e^2}{2 \sin^2 \theta_W} \frac{1}{s - M_Z^2} \bar{v}(p_2) \{ (-\not{p}_3 + \not{p}_4) \varepsilon^*(p_3) \cdot \varepsilon^*(p_4) \\
 &\quad - 2p_4 \cdot \varepsilon^*(p_3) \not{\varepsilon}^*(p_4) + 2p_3 \cdot \varepsilon^*(p_4) \not{\varepsilon}^*(p_3) \} (L + R) u(p_1), \\
 A^{d_-} &= -\frac{g^2}{2} \frac{1}{t - M_{d_-}^2} \bar{v}(p_2) \not{\varepsilon}^*(p_4) P_L (\not{t} - M_{d_-}) \not{\varepsilon}^*(p_3) P_L u(p_1),
 \end{aligned}$$

where $L = (1 - \frac{4}{3} \sin^2 \theta_w) P_L$, $R = -\frac{4}{3} \sin^2 \theta_W P_R$, θ_W is the weak mixing angle, and $P_L = \frac{1-\gamma_5}{2}$ ($P_R = \frac{1+\gamma_5}{2}$) is the left-handed (right-handed) projection operator. In the center-of-mass frame of $W_H^+ W_H^-$, the 4-momenta of the particles can be chosen to be

$$\begin{aligned}
 p_1 &= (E, 0, 0, E), \quad p_2 = (E, 0, 0, -E), \\
 p_3 &= (E, p \sin \theta, 0, p \cos \theta), \quad p_4 = (E, -p \sin \theta, 0, -p \cos \theta),
 \end{aligned}$$

where E is the energy of incoming and outgoing particles, p is the momentum of outgoing heavy gauge bosons and θ is the scattering angle. In order to check its high energy behavior, we consider the case that both the heavy gauge bosons W_H^+ and W_H^- are longitudinally

polarized. Since the incoming fermion u and anti-fermion \bar{u} have opposite helicities, the helicity amplitudes of s-channel and t-channel processes can be easily found to be

$$\begin{aligned} A^\gamma(-+) &= \frac{8e^2 E p(p^2 - 3E^2)}{3sM_{W_H}^2} \sin \theta, \\ A^Z(-+) &= (1 - \frac{4}{3}s_W^2) \frac{e^2}{s_W^2(s - M_Z^2)} \frac{2Ep(p^2 - 3E^2)}{M_{W_H}^2} \sin \theta, \\ A^{d-}(-+) &= \frac{e^2}{s_W^2(t - M_{d-}^2)} \frac{E(2E^3 \cos \theta + p^3 - 3pE^2)}{M_{W_H}^2} \sin \theta, \end{aligned}$$

where $s_W \equiv \sin \theta_W$, $(-+)$ are the helicities of $(u \bar{u})$, the Mandelstam variables $s \equiv (p_1 + p_2)^2$ and $t \equiv (p_1 - p_3)^2$, and M_Z , M_{W_H} and M_{d-} are the masses of Z -boson, heavy W -boson and heavy T-odd down-quark, respectively. As we take the high energy limit, i.e. $\sqrt{s} \gg M_X$ ($X = Z, W_H$ and d_-), each amplitude behaves as follows:

$$A^\gamma(-+) = -\frac{s_W^2 \sin \theta}{3f^2} s, \quad (25)$$

$$A^Z(-+) = -(1 - \frac{4}{3}s_W^2) \frac{\sin \theta}{4f^2} s, \quad (26)$$

$$A^{d-}(-+) = \frac{\sin \theta}{4f^2} s. \quad (27)$$

It is evident that each term diverges as energy goes to infinity, but their sum is zero because of the cancellation between the s-channel and t-channel contributions. Therefore, we conclude that including the contribution from the T-odd down-quark is essential to warrant a good high energy behavior of the scattering process $u\bar{u} \rightarrow W_H^+ W_H^-$. This can be illustrated by partial-wave analysis, as to be given below.

The $J = 1$ partial-wave amplitude (denoted as $a^{J=1}$) of the $u\bar{u} \rightarrow W_H^+ W_H^-$ process, for producing longitudinal W_H 's, consists of two contributions: one from s-channel, another from t-channel. We find

$$\begin{aligned} a_{\text{s-channel}}^{J=1} &= \frac{\alpha s}{48\sqrt{2}s_W^2 M_{W_H}^2} \beta(3 - \beta^2), \\ a_{\text{t-channel}}^{J=1} &= \frac{\alpha s}{64\sqrt{2}s_W^2 M_{W_H}^2} \int_{-1}^1 \frac{\sin^2 \theta (2 \cos \theta + \beta^3 - 3\beta)}{1 - \beta \cos \theta + \frac{2M_{d-}^2}{s}} d \cos \theta, \end{aligned}$$

where $\alpha = \frac{e^2}{4\pi}$ and $\beta \equiv \sqrt{1 - 4M_{W_H}^2/s}$. (e is the unit of electric charge.) When $s \gg M_{W_H}^2$ and $s \gg M_{d-}^2$, we have

$$a_{\text{s-channel}}^{J=1} = -a_{\text{t-channel}}^{J=1} = \frac{\alpha s}{24\sqrt{2}s_W^2 M_{W_H}^2}. \quad (28)$$

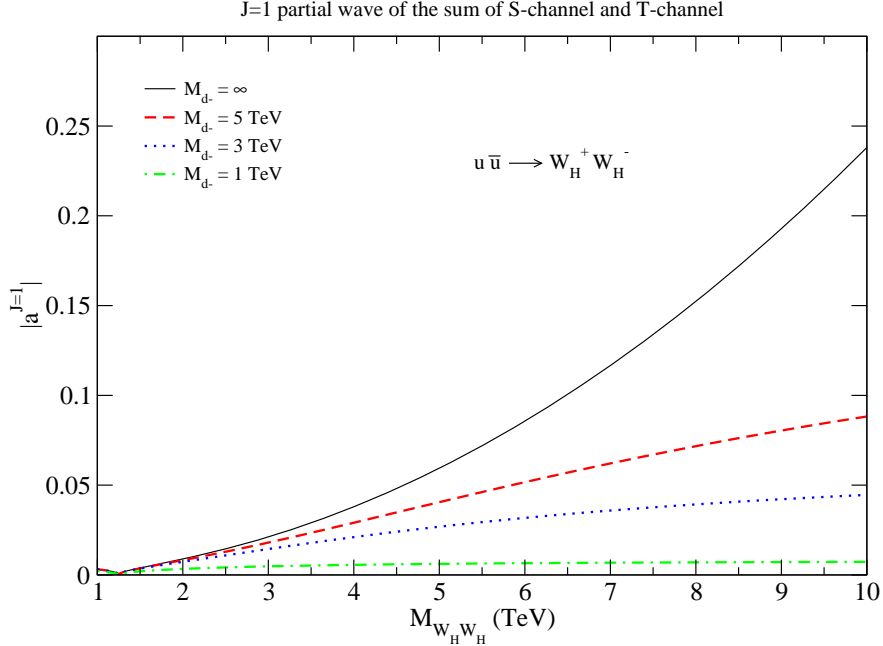


FIG. 3: $J = 1$ partial-wave amplitude of the $u\bar{u} \rightarrow W_H^+ W_H^-$ process, as a function of $M_{W_H W_H} (= \sqrt{s})$. The plots are shown for $M_{d_-} = 1, 3, 5 \text{ TeV}$ and ∞ .

In Fig. 3, we show the $J = 1$ partial-wave amplitude of the $u\bar{u} \rightarrow W_H^+ W_H^-$ process, as a function of the invariant mass (\sqrt{s}) of the $W_H^+ W_H^-$ pair, for cases with $M_{d_-} = 1, 3, 5 \text{ TeV}$ and ∞ . We found that the unitarity is not violated up to about 15 TeV in the decoupling limit of the T-odd down quark, i.e. $M_{d_-} \rightarrow \infty$. On the other hand, the constraint on the four-fermi operator contributing to the $e^+ e^- \rightarrow q\bar{q}$ scattering sets an important upper limit on the T-odd fermion mass, as shown in Eq. (10), thus the decoupling limit of the T-odd fermions is not a realistic assumption and the T-odd fermion contribution generates an important correction to $u\bar{u} \rightarrow W_H^+ W_H^-$ process. This contribution was not taken into account in the previous study [6]. As we show later, the theoretical prediction of the pair production cross section of heavy W -boson significantly depends on the mass of the T-odd down-quark. Moreover, because the mass of the T-odd $SU(2)$ doublet fermions cannot be too heavy, cf. Eq. (10), they can be copiously produced at the LHC. Therefore, in the following section, we study the collider phenomenology of the LHT with emphasis on the contributions of the T-odd fermion to the production of the heavy T-parity partners (either bosons or fermions) at the LHC.

IV. PHENOMENOLOGY

The Little Higgs mechanism which provides the cancellation of dominant quadratic divergences from the top-quark and SM gauge bosons in Higgs boson mass term, demands the presence of the partners to SM fermions and bosons. In particular, detection of the T-even and T-odd partners of top quark would provide a clear hint for the Little Higgs mechanism with T-parity. Similarly, the heavy T-odd gauge bosons of the electroweak gauge boson partners are also essential components of the Little Higgs mechanism. Many studies [6, 12, 17, 18, 19, 20, 21, 22, 23] have been presented in the literature on the detection strategies for T-even and/or T-odd partners of top quark and heavy T-odd gauge bosons at high energy colliders. On the other hand, the T-odd $SU(2)$ partners of SM fermions of the first and second generations received so far little attention with respect to collider phenomenology. As we have shown, these fermions are crucial component of LHT for providing its consistency with respect to unitarity and viability with respect to constraints from contact interactions.

In this section, we first discuss the production of these heavy T-odd fermions, either produced in pairs or in association with heavy T-odd gauge bosons at the LHC. Then, we discuss the impact of T-odd fermion contribution to the production of heavy T-odd gauge boson pairs. As discussed in the previous section, it is necessary to include the contribution from these heavy T-odd fermions to yield an unitary scattering amplitude. For completeness, we will also discuss the production of heavy T-odd triplet Higgs bosons. In the end of this section, we will briefly discuss the potential of the LHC for testing LHT by classifying several most interesting experimental signatures.

A. Direct Production Rates at the LHC

Given the model described in section II, we can easily calculate the direct production rates of non-SM fermions, gauge bosons and triplet Higgs bosons. In our numerical results, we have used CTEQ6M parton distribution functions [24] with the renormalization and factorization scales chosen to be the invariant mass of the constituent process. Only the leading order results are reported here. For our phenomenological analysis we have im-

plemented the complete LHT into CalcHEP package [25]⁴ and used it in our analysis. To check our analytical derivation of the effective lagrangian for the implementation of the LHT into CalcHEP, we applied LanHEP package [26] for automatic generations of Feynman rules for the CalcHEP. Indeed, it turned out that independent implementation of the model was crucial for the cross check of the previous studies [6].

In our analysis we fix the model parameters to be $\kappa = 1$, $s_\alpha = 1/\sqrt{2}$ (or equivalently, $\lambda_1 = \lambda_2 \sim \frac{\sqrt{2}M_t}{v_{SM}} \sim 1$), the Higgs boson mass $M_H=120$ GeV, and the top-quark mass $M_t = 175$ GeV, while studying the signal production rates as a function of the new particle mass scale f . With this choice of the model parameters, the effective $W^+ \bar{t} b$ coupling is $\frac{g}{\sqrt{2}} V_{tb}^{eff} \gamma_\mu P_L$ with $V_{tb}^{eff} = c_L = \sqrt{1 - s_L^2} \simeq 1 - 0.008 \left(\frac{1 \text{ TeV}}{f} \right)^2$.

1. Quark-Quark production rates

The LHC is a proton-proton hadron collider, so that a heavy T-odd quark, denoted as q_- can be copiously produced in pairs as long as its mass is not too large. There are two main mechanisms of T-odd quark pair production. Firstly, $q_- q_-^{(\prime)}$, same-sign-charge quarks can be produced via exchanging the T-odd heavy photon and Z-boson (A_H and Z_H) in t (or u)-channel processes initiated by same-sign-charge light quarks. A respective Feynman diagram corresponding to this process is shown in Fig. 4. Secondly, $q_- \bar{q}_-^{(\prime)}$ pair production takes place via both electroweak and obviously dominating QCD processes. The respective QCD Feynman diagrams for this process are shown in Fig. 5.

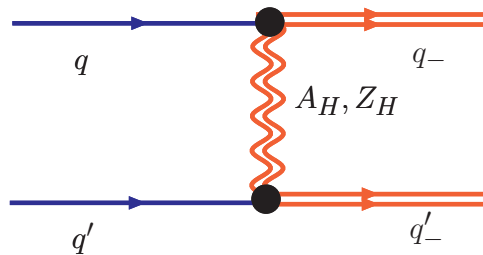


FIG. 4: Representative Feynman diagram for $pp \rightarrow q_- q_-^{(\prime)}$ via t-channel exchange of T-odd photon A_H and T-odd Z-boson Z_H .

⁴ We are grateful to Alexander Pukhov for developing new CalcHEP version while visiting Michigan State University.

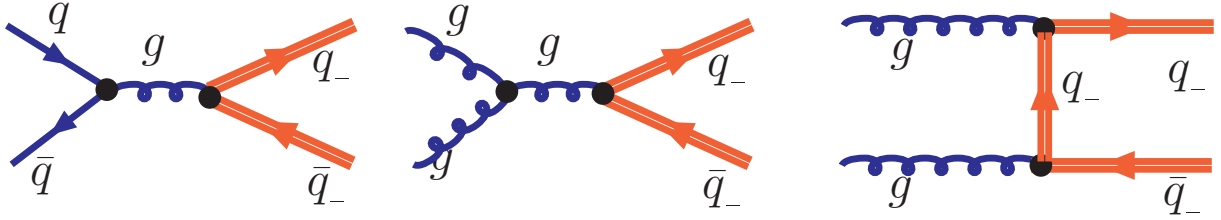


FIG. 5: QCD Feynman diagrams for $pp \rightarrow q_- \bar{q}_-$ process.

In Fig. 6 we present pair production rates of first and second generation heavy T-odd quarks versus f value, organized by their electric charges. The corresponding masses of the new heavy particles relevant to the production processes under consideration are listed in the top margin of the figure, corresponding to the respective f values at the bottom. For example, in Fig. 6, for $f = 1$ TeV one has $M_{q_-} \simeq 1.4$ TeV, $M_{W_H} \simeq 0.65$ TeV and $M_{A_H} \simeq 0.15$ TeV.

The solid curve presents the production cross section of heavy quark pairs with positive charges, $q_-^+ q_-^+$, which includes, for example, $u_- u_-$, $\bar{d}_- \bar{d}_-$ and $u_- \bar{d}_-$ pairs. The dashed curve is for the production of heavy quark pairs with negative charges, $q_-^- q_-^-$, which includes, for example, $\bar{u}_- \bar{u}_-$, $d_- d_-$ and $d_- \bar{u}_-$ pairs. The dot-dashed curve is for the production of heavy quark pairs with opposite-sign charges, $q_-^+ q_-^-$, which includes, for example, $u_- d_-$ and $\bar{u}_- \bar{d}_-$ pairs. It is evident that the heavy T-odd quark pair production rates are sizable. The production rate of positive charge pairs is larger than that of the negative charge pairs because of the larger parton density associated with positive charge pair production in proton-proton collision. One should notice that electroweak $q_-^+ q_-^+$ production is comparable with essentially QCD $q_-^+ q_-^-$ production! This happens because the production of heavy quark pairs with positive charges is initiated by both valence quarks in the proton which have higher parton density than that contributing to either QCD or EW $q_-^+ q_-^-$ production. Furthermore, $q_-^+ q_-^+$ ($q_-^- q_-^-$) production becomes even more sizable as compared to $q_-^+ q_-^-$ production when f (and so the T-odd quark mass) increases, since the contribution from valence quarks becomes more important in the large x -value region. This is an important result because the $q_-^+ q_-^+$ ($q_-^- q_-^-$) production can provide an exciting experimental signatures at the LHC, as we shall discuss together with their detection strategies in the following subsections.

In Fig. 7 we present various production rates of heavy T-even and T-odd top quark pairs

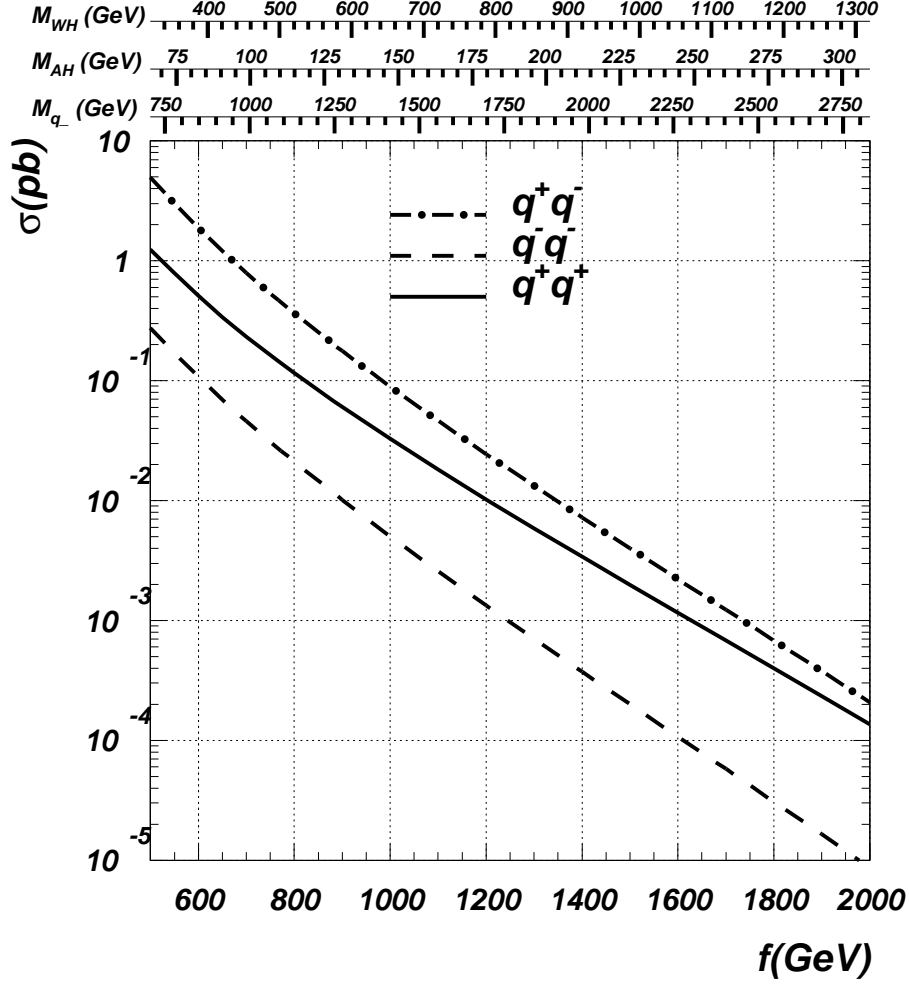


FIG. 6: The first and second generation heavy T-odd quark production cross sections at the LHC, where $q^+ = \{u_-, c_-, \bar{d}_-, \bar{s}_-\}$ and $q^- = \{\bar{u}_-, \bar{c}_-, d_-, s_-\}$. The solid curve presents the production cross section of heavy quark pairs with positive charges ($q^+_+q^+_+$), dashed curve is for the production of heavy quark pairs with negative charges ($q^-_-q^-_-$) and dot-dashed curve is for the production of heavy quark pairs with opposite-sign charges ($q^+_+q^-_-$). The corresponding masses of the new heavy particles relevant to the production processes under consideration are listed in the top margin of the figure, corresponding to the respective f values at the bottom.

as well as the rate of single T-even heavy top quark associatively produced with SM light quarks as a function of f . The T-odd bottom quark pair production rate is also given.

The T-odd heavy singlet top quark pairs ($T_-\bar{T}_-$) have the largest cross section (solid curve) because in the LHT, considered here, the T-odd heavy singlet top quark (T_-) is

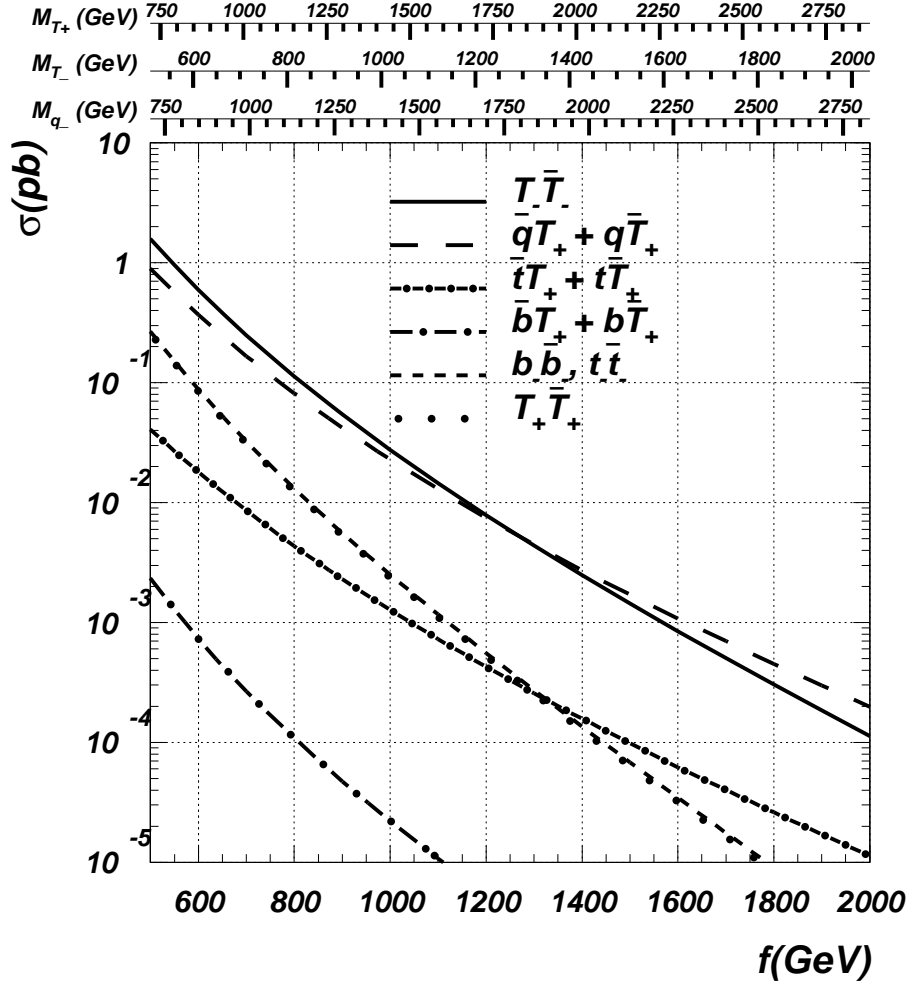


FIG. 7: The third generation heavy T-odd and T-even quark production cross sections at the LHC.

lighter than the T-even heavy top (T_+). Note that the mass of T-odd doublet quarks is determined by the choice of κ value which is taken to be 1. In this case T-odd heavy doublet top quark (t_-) mass is larger than the T_- mass and is about the same as the T_+ mass.

As f increases, both T_- and T_+ become heavier, and the single- T_+ production in association with light quarks ($\bar{q}T_+ + q\bar{T}_+$) (long-dashed curve) rate becomes larger than the $T_- \bar{T}_-$ rate. This is because of the phase space suppression in $T_- \bar{T}_-$ (or $T_+ \bar{T}_+$ - dotted curve) pair production, for producing two heavy particles, as compared to producing only one heavy particle in single- T_+ event. Furthermore, the single- T_+ production mechanism is dominated by longitudinal W -boson fusion with the incoming bottom quark in the t -channel production

process, similar to the SM t-channel single-top production [27, 28]. Due to the collinear enhancement for the light quark emitting a W -boson in the high energy region, the constituent cross section of single- T_+ process does not drop as fast as that of pair production process. We note that for a fixed T_+ mass, the single- T_+ production rate is proportional to s_α^2/c_α^2 . This is because the coefficient of $W^+\bar{T}_+b$ coupling is $V_{tb}^{eff} \frac{s_L}{c_L} \sim V_{tb}^{eff} s_\alpha^2 \frac{v_{SM}}{f} \simeq V_{tb}^{eff} \frac{s_\alpha}{c_\alpha} \frac{M_t}{M_{T_+}}$, cf. Appendix A. In Fig. 7, we also show the production rates of the T-odd $t_-\bar{t}_-$ and $b_-\bar{b}_-$ pairs (short-dashed curve), where t_- and b_- are originated from the T-odd $SU(2)$ doublet quark fields, and their masses are generated from the κ term of the effective Lagrangian. One can see that $T_+\bar{T}_+$ and $t_-\bar{t}_-$ (or $b_-\bar{b}_-$) production cross sections are very close to each other because of the same production mechanism and the similar masses of T_+ and t_- (b_-) (for this particular choice of model parameters). Fig. 7 also presents cross sections for the associate tT_+ (short dot-dashed line) and bT_+ (long dot-dashed line) productions. The tT_+ production rate dominates over the bT_+ rate because the diagram with t-channel W -boson exchange plays the leading role for the tT_+ production, and the similar diagram for bT_+ production is suppressed by CKM matrix elements. For example, it is suppressed by V_{cb} in the $cb \rightarrow bT_+$ production process.

2. Quark-Boson production rates

Another production mechanism for heavy T-odd quarks in the LHT is via associated production with heavy T-odd gauge bosons. Since the initial state of the scattering processes is T-even, the final state has to be a pair of T-odd particles. For example, the $d_-W_H^+$ pair can be produced via the $ug \rightarrow d_-W_H^+$ production. In Fig. 8, we show the associated production rates of heavy T-odd gauge bosons with all possible T-odd heavy quarks and anti-quarks, including the T-odd partner of heavy top (anti-) quark, as a function of f value. The fractional contribution from $t_-W_H^-$ (and $\bar{t}_-W_H^+$), initiated by an incoming b -quark, to the $q_-W_H^-$ production is at the percent level, because of the smallness of b -quark parton density inside the proton. Similarly, the fractional contribution from b_-Z_H (and \bar{b}_-Z_H) to the q_-Z_H production is also at the percent level, while the t_-Z_H contribution is not included because we do not take top quark as a parton in our calculation. The same conclusion for q_-Z_H production also holds for q_-A_H production after substituting Z_H by A_H .

One can see that q_-W_H (solid line) associate production is the dominant one, q_-Z_H

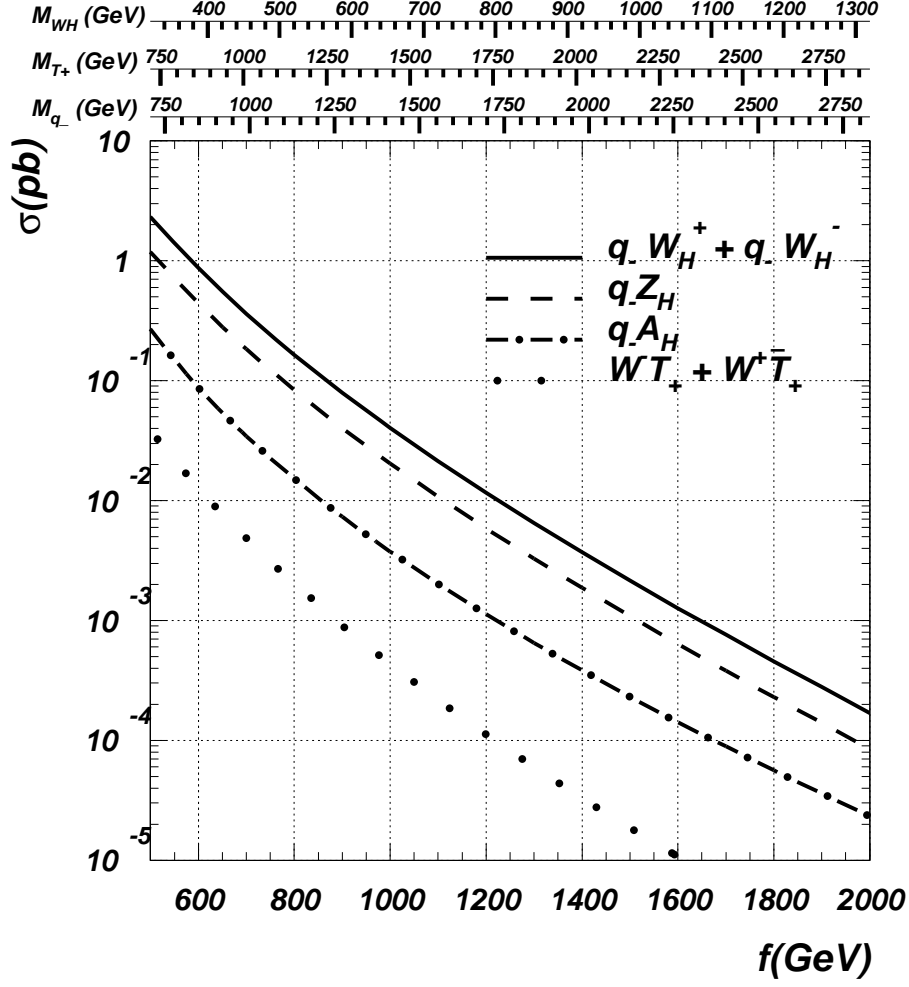


FIG. 8: Heavy quark-boson associated production rates at the LHC.

(dashed line) production rate is about a factor of 2 smaller due to the ratio in their couplings $|g_{qq-W_H}/g_{qq-Z_H}| \simeq \sqrt{2}$, and $q-A_H$ (dot-dashed line) production is suppressed even more due to $|g_{qq-W_H}/g_{qq-A_H}| \simeq 5\sqrt{2} \cot \theta_W$.

We note that due to T-parity, the T-even heavy top quark T_+ can be produced associatively with the SM (hence, T-even) gauge bosons, not the T-odd heavy gauge bosons, whose production rates are also given in Fig. 8 (dotted line). Since bT_+W coupling is suppressed as v/f , one can see that T_+W^- (\bar{T}_+W^+) rate is significantly smaller than the $q-W_H$ rate, and this suppression obviously grows with the increase of f value.

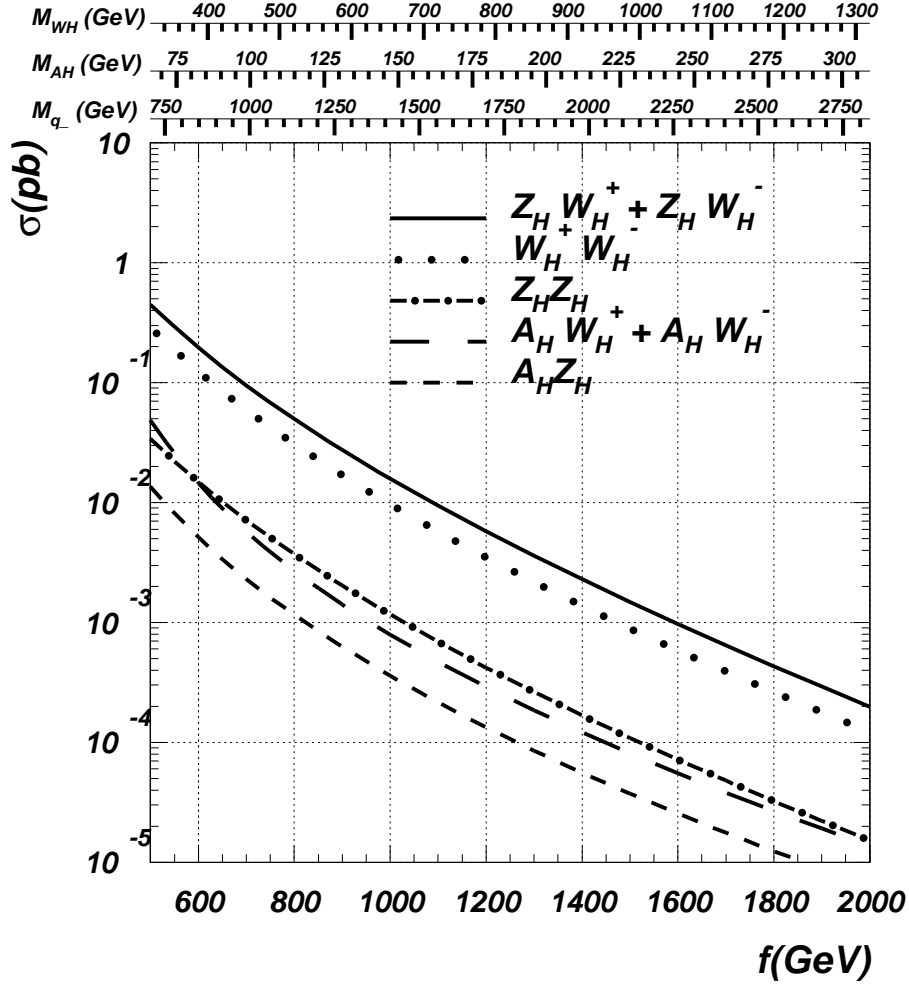


FIG. 9: Heavy T-odd gauge boson pair production rates at the LHC.

3. Boson-Boson production rates

As discussed in the previous section, the presence of the T-odd heavy quarks in the model is essential for unitarising the scattering amplitudes of $qq \rightarrow V_H V_H$ processes, where V_H denotes T-odd heavy electroweak gauge bosons. In Fig. 9 we show all possible T-odd heavy gauge boson pair production cross sections versus f values. We note that due to the destructive effect from the t-channel T-odd heavy quark exchange diagram, which is needed to respect unitarity in high energy region, the predicted T-odd gauge boson pair production rates are smaller than those reported in Ref. [6] where the important T-odd heavy quark exchange diagram was not included in the calculations.

Moreover, it is not a constant suppression factor in every production channel such that the

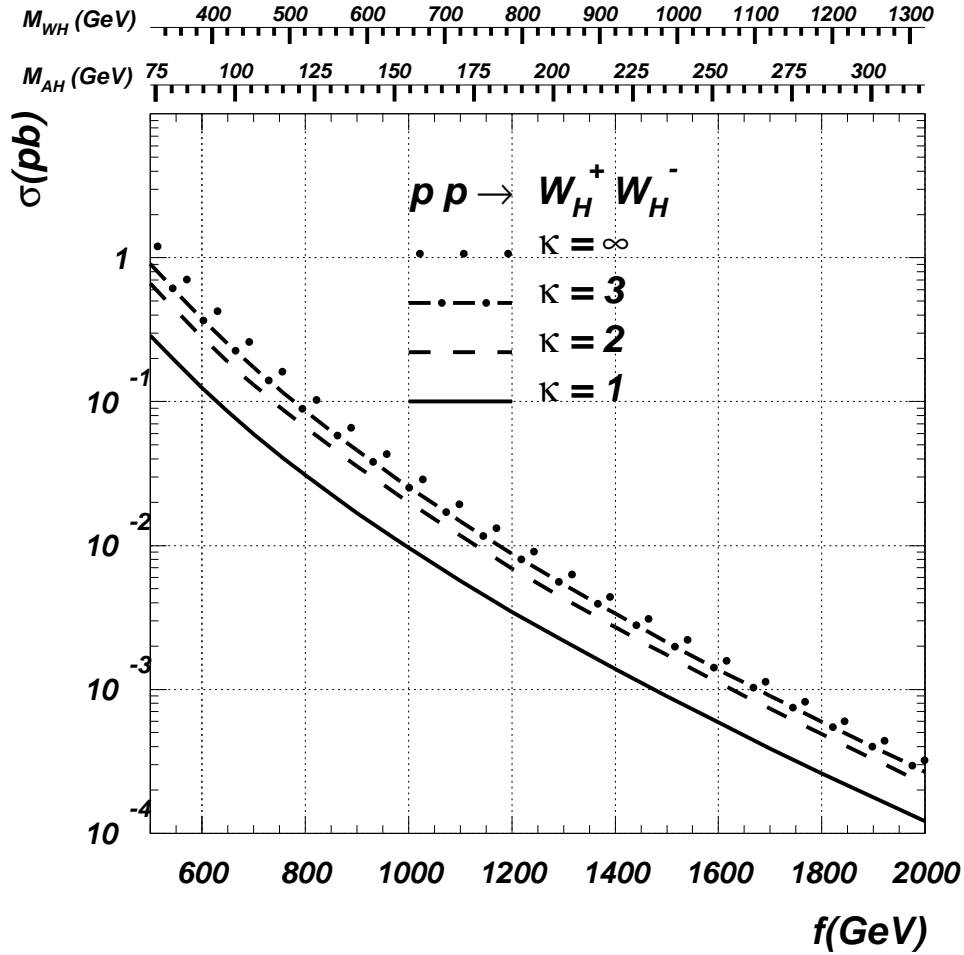


FIG. 10: Heavy T-odd gauge boson pair, $pp \rightarrow W_H^+ W_H^-$, production rates at the LHC.

relative difference between the $Z_H W_H^\pm$ and $W_H^+ W_H^-$ rates is much smaller than that reported in Ref. [6]. To examine the dependence on model parameters, we show in Fig. 10 the production cross section of $W_H^+ W_H^-$ pair at the LHC as a function of f for various choices of κ values. We note that the curve for $\kappa \rightarrow \infty$ corresponds to the calculation without including the T-odd heavy quark contribution which overestimates $W_H^+ W_H^-$ production rate by a significant factor. In the later section, we shall come back to discuss its detection strategies at the LHC.

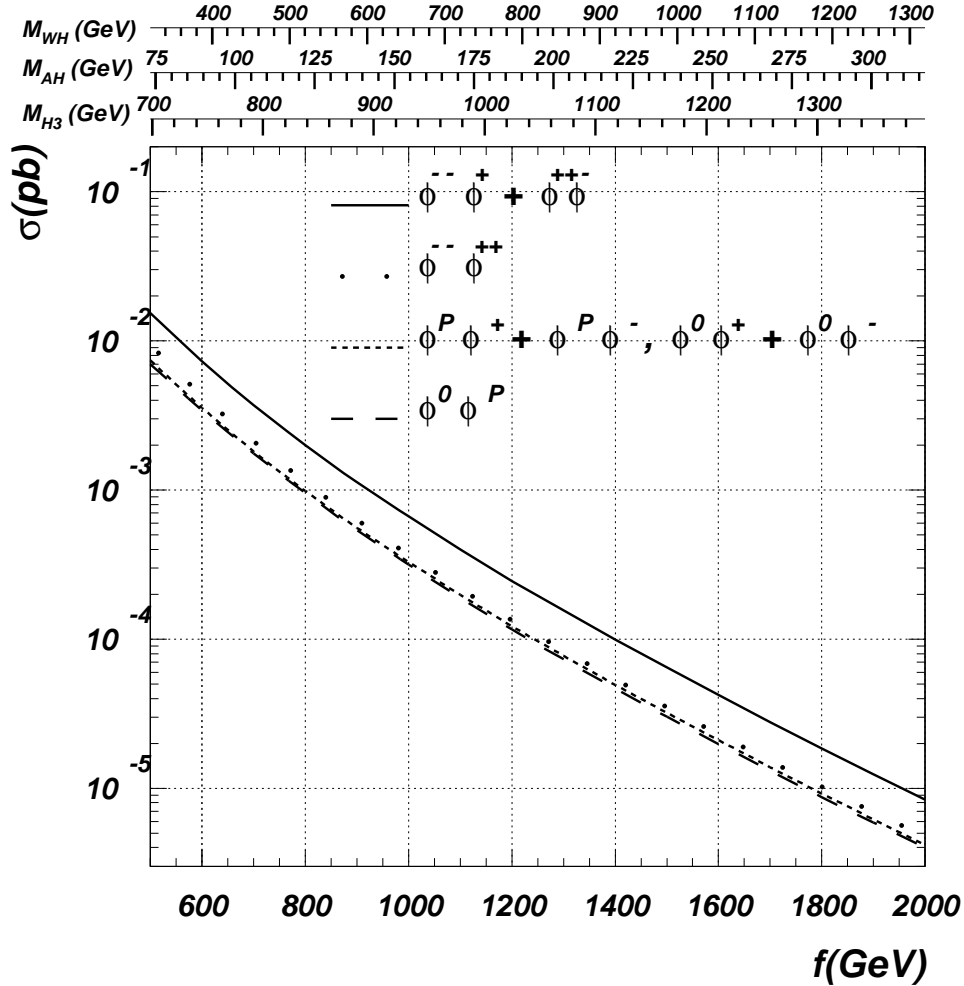


FIG. 11: Heavy T-odd Higgs production rates at the LHC.

4. Higgs-Higgs production rates

In the LHT, the direct production mechanism of the normal (T-even) Higgs boson is similar to the SM Higgs boson production though with somewhat suppressed couplings. We refer the reader to Ref. [16] for more detailed discussions. In high energy collision, the T-odd triplet Higgs bosons can be produced in $qq \rightarrow \phi\phi$ processes at the tree level via gauge interactions of ϕ , where ϕ denotes any of the T-odd heavy triplet Higgs bosons. Their direct production rates are small because at tree level they are produced via s-channel processes with highly virtual gauge boson propagators. Though t-channel diagrams also take place, they are strongly suppressed because they involve heavy T-odd quarks and the $qq\text{-}\phi$ coupling is suppressed at least by v/f .

Particle	Decay Mode	Branching Ratio(%)	Particle	Decay Mode	Branching Ratio(%)
u_-	$W_H^+ d$	61	d_-	$W_H^- u$	62
	$Z_H u$	30		$Z_H d$	31
	$A_H u$	8.6		$A_H d$	6.3
b_-	$W_H^- t$	60	t_-	$W_H^+ b$	62
	$Z_H b$	32		$Z_H t$	29
	$A_H b$	6.6		$A_H t$	8.2
T_-	$A_H t$	100	T_+	$W^+ b$	46
				$Z t$	22
				$H t$	20
				$A_H T_-$	12
W_H^+	$A_H W^+$	100	Z_H	$A_H H$	100
ϕ^+	$A_H W^+$	100	ϕ^0	$A_H Z$	100
ϕ^p	$A_H H$	100			

TABLE III: Decay branching ratio of heavy particles in Littlest Higgs Model with T-parity. Values in this table are calculated with parameters $\kappa = 1$, $f = 1$ TeV, $M_H = 120$ GeV and $M_t = 175$ GeV. We notice that for this set of model parameter values, the triplet Higgs ϕ^{++} doesn't have two-body decay modes at tree level.

Nevertheless, the T-even Higgs bosons can be copiously produced from the decay of T-odd heavy quarks, as to be discussed below. For that, we shall first examine the decay branching ratios of the T-odd heavy quarks and gauge bosons predicted in this model.

B. Decay branching ratios

In order to study the phenomenology of the T-odd heavy particles predicted in the LHT, we need to know about their decay branching ratios. In addition to the SM parameters, the dominant two-body decay modes of the first and second generation T-odd quarks only depend on two more parameters: f and κ , i.e. f determines the mass of the T-odd heavy gauge bosons and both f and κ determine the mass of T-odd heavy quarks. If κ is of the order of 1, then because of the smallness of gauge coupling strength, the T-odd gauge bosons are typically lighter than the T-odd quarks. When the lightest T-odd particle (LTP) is A_H so that it could be a good candidate for dark matters, the heavy T-odd quarks mainly decay into a normal QCD jet plus a T-odd heavy gauge boson W_H^\pm , Z_H or A_H . As shown in Table III, the decay branching ratio (BR) into $W_H^\pm + jet$ is about twice of $BR(Z_H + jet)$ and one order of magnitude larger than $BR(A_H + jet)$ for $f = 1$ TeV and $\kappa = 1$. This feature also holds for the T-odd heavy top (t_-) and bottom (b_-) quarks which are originated from

the T-odd $SU(2)$ doublet quark fields and gain their masses from κ terms. The T-odd heavy $SU(2)$ singlet top quark (T_-), originated from the top quark Yukawa interaction Lagrangian, decays almost 100% into the tA_H mode. The T-even heavy $SU(2)$ singlet top quark (T_+) has a more complicated decay pattern and can decay into W^+b , Ht , Zt and $A_H t_-$ modes with nontrivial dependence on the model parameters such as f , λ_1 and λ_2 (or, equivalently, the masses of heavy T-odd gauge bosons, T_+ and T_-). In Fig. 12, we present the decay branching ratios for the above decay channels of T_+ as a function of c_α (left frame) for $f=1$ TeV, and as a function of f for $s_\alpha = 1/\sqrt{2}$ (right frame) ⁵. One can see that at $c_\alpha \simeq 1$, $\text{BR}(T_+ \rightarrow Ht)$ becomes dominant since for small s_α , HT_+t coupling is proportional to c_α while the couplings of T_+ in the other decay channels are suppressed by s_α . Note that for our analysis, the coefficient of the $W^+\bar{t}b$ coupling $V_{tb}^{eff} \equiv V_{tb}c_L$ varies as c_L , cf. Appendix A. Here V_{tb} is taken to be 1. On the other hand, the BR of T-odd heavy quarks are quite insensitive to the LHT parameters as long as the mass of the T-odd heavy quark is larger than A_H . For example, the values of BRs shown in Table III also hold (within a few percents) for $f = 0.5 - 1$ TeV range. Hereafter, we will take $f = 1$ TeV as the reference point.

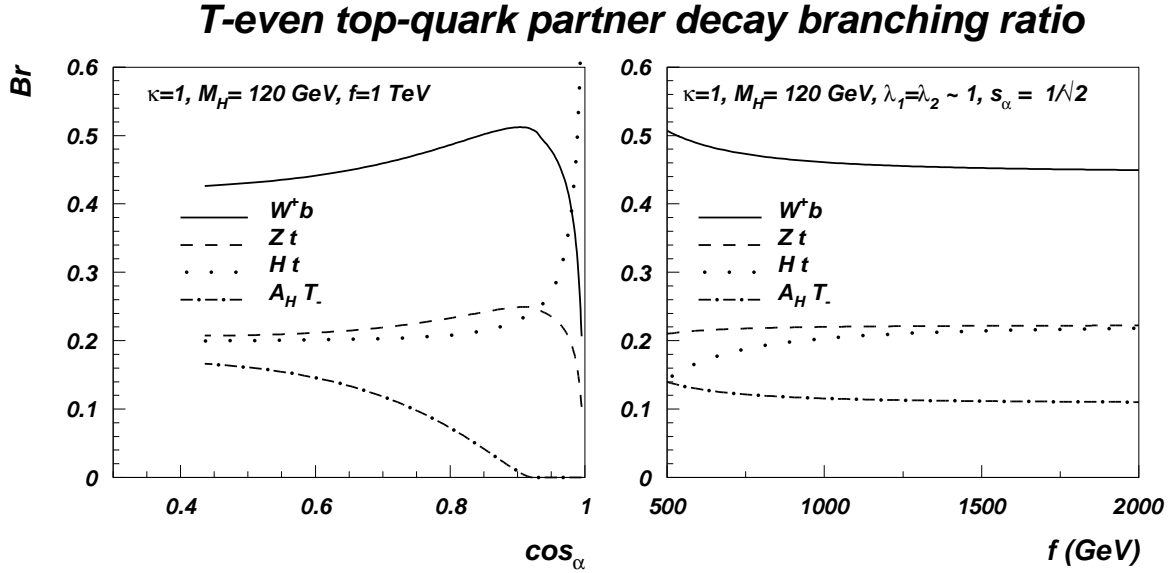


FIG. 12: T-even heavy top decay branching ratios for $\kappa = 1$, $\lambda_1 = \lambda_2$ (or, $s_\alpha = 1/\sqrt{2}$) and $M_H = 120$ GeV.

⁵ We have found disagreement for branching ratios of T_+ for small values of s_α as compared to results reported in Ref. [6]. In our paper, c_α corresponds to s_λ of Ref. [6]. For the sake of comparison we present c_α dependence of $\text{BR}(T_+)$ in the left frame of Fig. 12.

The striking feature of the T-odd heavy gauge boson decay pattern is that W_H^\pm almost exclusively decay into a $W^\pm A_H$ pair, while Z_H decays into a ZH pair, for κ being of the order 1 and the mass of the (T-even) Higgs boson is about 120 GeV. This is because the masses of W_H^\pm and Z_H are about the same and are smaller than the T-odd heavy quark masses (unless κ is much less than 1). In such cases, the normal (T-even) Higgs boson can be copiously produced from the decay of T-odd heavy gauge boson Z_H which can be produced either associatively with T-odd heavy quarks or another heavy T-odd gauge bosons, as discussed above.

For the chosen model parameters, with $\kappa = 1$ and $\lambda_1 = \lambda_2$ (or, $s_\alpha = 1/\sqrt{2}$) and $M_H = 120$ GeV, there is no tree-level two-body decay mode for the T-odd doubly charged triplet Higgs boson, $\phi^{\pm\pm}$, while ϕ^\pm decays into $W^\pm A_H$ mode, and ϕ^0 and ϕ^P decay into ZA_H and HA_H modes, respectively. However, for $M_H \geq 130$ GeV, the $W_H^\pm W^\pm$ mode could be opened for $\phi^{\pm\pm}$ Higgs boson.

C. Signal processes and the collider signatures

In this section we shall discuss various experimental signatures of signal processes at the LHC for the same values of model parameters as given in the previous section. For simplicity, we shall concentrate on the pure leptonic decay modes of gauge bosons in the final decay chain of T-odd heavy quarks and gauge bosons.

1. The 1st and 2nd generation heavy T-odd quark pair production

According to the multiplicity and charge of the leptons produced from the first and second generation T-odd heavy quark chain decays, we can classify the T-odd heavy quark pair event signature as signal events with like-sign di-leptons, opposite-sign di-leptons, and single charged lepton with large missing transverse momentum.

1) like-sign di-lepton ($\ell^\pm \ell^\pm + \cancel{E}_T + jets$) signature (LSL)

As shown in Fig. 4, the valence quark initiated $pp \rightarrow q_- q_-$ processes via the exchange of heavy electroweak gauge bosons could give rise to a large production rate of signal events with a pair of like-sign charged leptons in the final state to yield a distinct experimental signature. For example,

$$u_- u_- \rightarrow W_H^+ d W_H^+ d \rightarrow W^+ W^+ A_H A_H d d \quad \text{and} \quad u_- \bar{d}_- \rightarrow W_H^+ d W_H^+ \bar{u} \rightarrow W^+ W^+ A_H A_H d \bar{u}$$

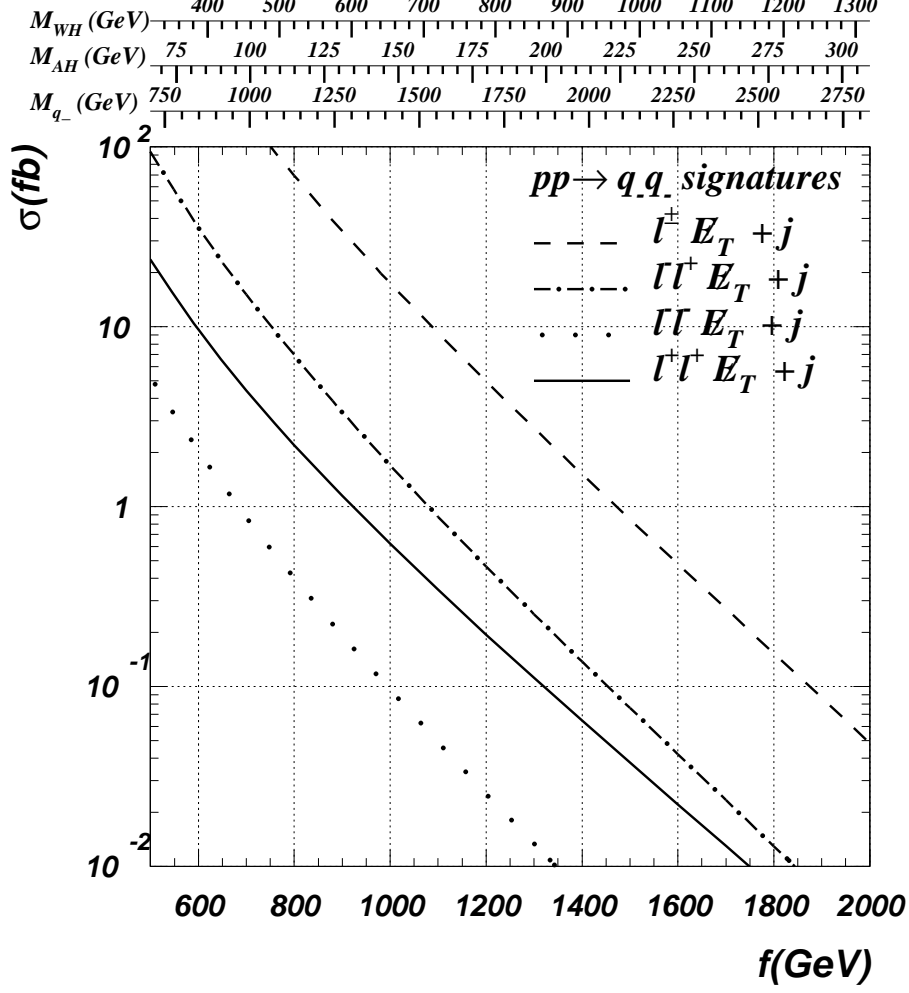


FIG. 13: Rates for like-sign di-lepton, opposite-sign di-lepton and single charged lepton signatures from the 1st and 2nd generation heavy T-odd quark pair production at the LHC.

chains lead to the $\ell^+\ell^+ + \cancel{E}_T + jets$ signature, while

$d_-d_- \rightarrow W_H^- u W_H^- u \rightarrow W^- W^- A_H A_H u u$ and $d_- \bar{u}_- \rightarrow W_H^- u W_H^- \bar{d} \rightarrow W^- W^- A_H A_H u \bar{d}$ processes produce $\ell^-\ell^- + \cancel{E}_T + jets$ final state.

The overall decay branching ratios for the above reactions can be easily calculated from Table III which yields $Br[q_-q_- \rightarrow LSL] = 0.62^2 \times (2/9)^2 \simeq 0.019$. Depending on the values of f , the LSL signal event rate for positively charged leptons is about at 23 fb level for a lower value of $f = 0.5$ TeV and about 0.6 fb for $f = 1$ TeV, as shown in Fig. 13. LSL signal event rate for negatively charged leptons is 5 fb and 0.1 fb, respectively, as shown by dotted line in Fig. 13.

With the high luminosity option of the LHC, around 300 fb^{-1} , there will be a large number

of signal events with like-sign di-leptons, with large transverse momentum (P_T), and large missing transverse momentum (\cancel{E}_T) in the $\ell^-\ell^- + \cancel{E}_T + jets$ or $\ell^+\ell^+ + \cancel{E}_T + jets$ signature. The prominent feature of this signal signature is that it is free of large $t\bar{t}$ background. This is similar to the case for studying the longitudinal weak boson scattering processes in the TeV region, with emphasis on the so called Gold-platted purely leptonic decay mode of weak bosons. As shown in Ref. [29], after imposing the kinematic cuts on the charged leptons, the SM background rate, which is dominated by the intrinsic electroweak $qqW^\pm W^\pm$ production and the $Wt\bar{t}$ associate production, is already down to the level of a few tenth fb. It is expected that one can further discriminate the signal event from the SM background event by requiring a large scalar sum of the transverse momenta, contributed by the two high P_T charged leptons, jets and \cancel{E}_T , which is known as the H_T parameter in the search for top quark at the Tevatron [30]. This is because in the signal event, two heavy T-odd quarks are produced so that the center-of-mass system has a much larger mass. Furthermore, one can use the kinematic constraints, similar to those used in the $t\bar{t}$ analysis carried out at the Tevatron, to purify the data sample with T-odd heavy quarks. Finally, one can construct the transverse mass of the final state system, in analogy to the one introduced in Ref. [29] for studying the longitudinal weak boson scattering, to further discriminate the SM background from the signal events. Therefore, the LSL signature of the T-odd quark pair events is expected to provide a clear verification or disproof of the Littlest Higgs model with T-parity unless the signal production rate is largely suppressed for very large f and therefore very heavy T-odd quarks.

2) opposite-sign lepton ($\ell^\pm\ell^\mp + \cancel{E}_T + jets$) signature (OSL)

As shown in Fig. 6, the production of T-odd heavy quark pairs with opposite electric charges has a higher rate than the like-sign heavy quark pairs. For example,

$$u_-\bar{u}_- \rightarrow W_H^+ d W_H^- \bar{d} \rightarrow W^+ W^- A_H A_H \bar{d} d,$$

$$u_- d_- \rightarrow W_H^+ d W_H^- u \rightarrow W^+ W^- A_H A_H d u,$$

$$d_- \bar{d}_- \rightarrow W_H^- u W_H^+ \bar{u} \rightarrow W^- W^+ A_H A_H u \bar{u},$$

$$d_- \bar{u}_- \rightarrow W_H^- u W_H^+ \bar{d} \rightarrow W^- W^- A_H A_H u \bar{d}$$

processes all give rise to the $\ell^+\ell^- + \cancel{E}_T + jets$ signature. When the mass of the T-odd heavy quarks increases, the electroweak production rate becomes more important than the QCD production rate. One of the reasons is that the former process is dominated by the t-channel exchange of a relative light A_H boson, and the later process is induced by the s-channel

exchange of a virtual gluon. Another reason is that the former process can be initiated by two valence quarks (via t-channel process) while the later process must involve a sea-quark parton whose density function becomes smaller in the large x -region for producing a heavier T-odd heavy quark pair.

The overall decay branching ratio for the above reactions is equal to $\text{Br}[q_-q_- \rightarrow LSL]$. Hence, the OSL signal event rate is larger than the LSL signal event rate as indicated by the dot-dashed line in Fig. 13. However, the OSL signal suffers from a much larger SM background rate induced by the $t\bar{t}$ production. Nevertheless, the same strategies discussed above to suppress the SM background rate in the LSL analysis also applies to the OSL case because the signal events are all generated from a system with a much larger mass (i.e., the invariant mass of the heavy T-odd quark pair) as compared to the SM background processes. To be certain, a detailed Monte Carlo analysis is needed which is beyond the scope of this work.

3) Single charged lepton ($\ell^\pm + \cancel{E}_T + jets$) signature (1L)

One may also consider the signal event signature with only one charged lepton in its final state, with one of W^\pm decaying leptonically and another hadronically. The overall decay branching for the above reactions is equal to $\text{Br}[q_-q_- \rightarrow 1L] = \text{Br}[q_-q_- \rightarrow W_H W_H qq \rightarrow 1L] + \text{Br}[q_-q_- \rightarrow W_H A_H qq \rightarrow 1L] = 0.62^2 \times 2/9 \times 2/3 \times 2 + 0.62 \times 0.086 \times 2/9 \times 2 \simeq 0.14 \simeq 6 \times \text{Br}[q_-q_- \rightarrow LSL]$. The production rate is also higher, as presented by the dashed line in Fig. 13, for all the above T-odd heavy quark pair production channels are combined. On the other hand, the expected background will also be orders of magnitude higher. Hence, it is more challenging to detect the signal events in the single charged lepton mode.

2. The third generation heavy quark pair production

In order to cancel the quadratic divergence induced by the top quark loop for Higgs boson mass correction at the one-loop order, we need to introduce additional heavy quarks (heavy partners of top quark) into the LHT model. In general, there are T_+ , T_- , originated from the top quark Yukawa sector, cf. Eq. (12), and t_- , originated from the κ term interaction with b_- as its isospin partner, cf. Eq. (8).

1) $T_- \bar{T}_-$ production with $T_- \bar{T}_- \rightarrow A_H A_H t \bar{t}$

The $T_- \bar{T}_-$ production rate at the LHC is quite large, which is about 30 fb for $f = 1$ TeV. The

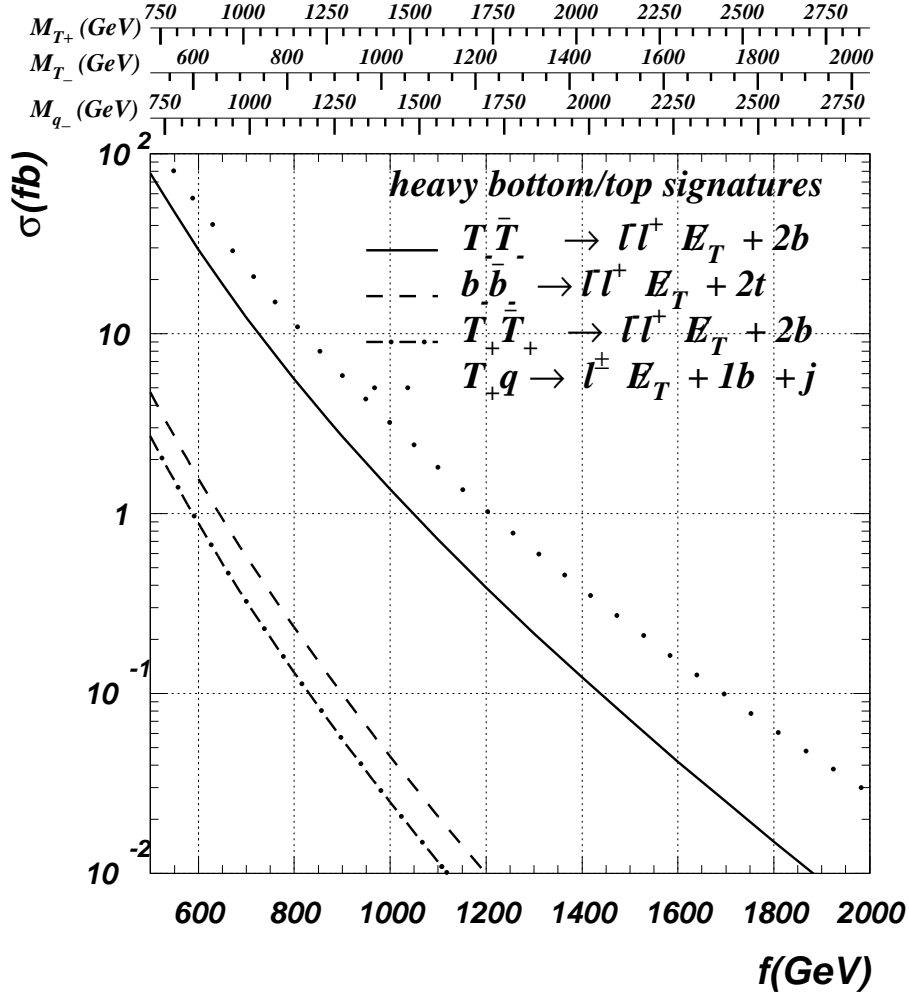


FIG. 14: Rates for opposite-sign di-lepton and single charged lepton signatures from the third generation heavy quark pair production at the LHC.

experimental signature of this signal event can be either OSL or 1L. Its production rate only depends on T_- mass and the decay branching ratio of $T_- \rightarrow t A_H$ is about 100%. Therefore, it is important to test this production mode at the LHC, for the signal rate can be predicted with great confidence. We present OSL rates for $T_- \bar{T}_-$ production in Fig. 14 as solid line. There have been a few studies in the literature to discuss how to detect this channel at the LHC [6, 21], though more detailed Monte Carlo analysis is needed to confirm how well this channel can be detected. It was also pointed out that it could be very challenging to distinguish this production channel with the top-squark (stop) pair productions predicted by the Minimal Supersymmetric Standard Model (MSSM) with the subsequent decay of stop into top quark and the lightest supersymmetric particle (neutralino) [21]. Needless to say

that distinguishing the LHT from the MSSM generally requires studying of all detectable experimental signatures induced by various production mechanisms predicted by the models.

2) $t_-\bar{t}_-$ and $b_-\bar{b}_-$ production

For the particular choice of $\kappa = 1$, which makes t_- and b_- heavier than T_- , the $t_-\bar{t}_-$ production rate is at least one order of magnitude (depending on the value of f) lower than the $T_-\bar{T}_-$ rate. In case of $t_-\bar{t}_-$ production, there will be two b -jets associatively produced with a pair of OSL or 1L in its event signature. Likewise, the $b_-\bar{b}_-$ process gives rise to a $t\bar{t}$ pair in addition to the OSL or 1L signature. The rate for OSL+ $t\bar{t}$ signature is presented in Fig. 14 by dashed line. The rate for OSL+ $b\bar{b}$ from $t_-\bar{t}_-$ production is very similar and is not shown. Depending on κ , $t_-\bar{t}_-$ production rate could be higher or lower than the $T_-\bar{T}_-$ production rate, making it, respectively, harder or easier to observe.

3) $T_+\bar{T}_+$ production

Since T_+ is heavier than T_- , the $pp \rightarrow T_+\bar{T}_+$ production rate (similar to the $t_-\bar{t}_-$ or $b_-\bar{b}_-$ production rate) is at least one order of magnitude lower than the $T_-\bar{T}_-$ production rate (depending on the value of f). The highest rates are for $T_+\bar{T}_+ \rightarrow W^+W^-b\bar{b}$ signature which should be checked against the SM $t\bar{t}$ background. The rate for OSL+ $b\bar{b}$ signature is presented in Fig. 14 by the dot-dashed line. Again, the techniques discussed about for using the large invariant mass of the heavy system in the signal event to distinguish it from the SM background event could be useful for detecting the signal event in this channel.

4) single T_+ production

The rate of single- T_+ production associated with a light quark via t-channel electroweak interaction is actually higher than the rate of $T_+\bar{T}_+$ pair production via strong interaction, as clearly shown in Fig. 7. The dominant experimental signature of the signal event is the same as the SM single-top event though it is expected with a much larger missing transverse momentum. In Fig 14 the dotted line presents the rate of 1L signature originated from the single T_+ production in association with the light quark. Furthermore, the transverse mass of the signal event will be larger than that of the SM single-top event. In analogy to the SM single-top event, the single- T_+q event is also characterized by a forward-jet which populates in the large rapidity region and can be used to suppress $t\bar{t}$ and $Wb\bar{b}$ backgrounds [27]. Again, a Monte Carlo study is needed to draw any definite conclusion about its detection at the LHC.

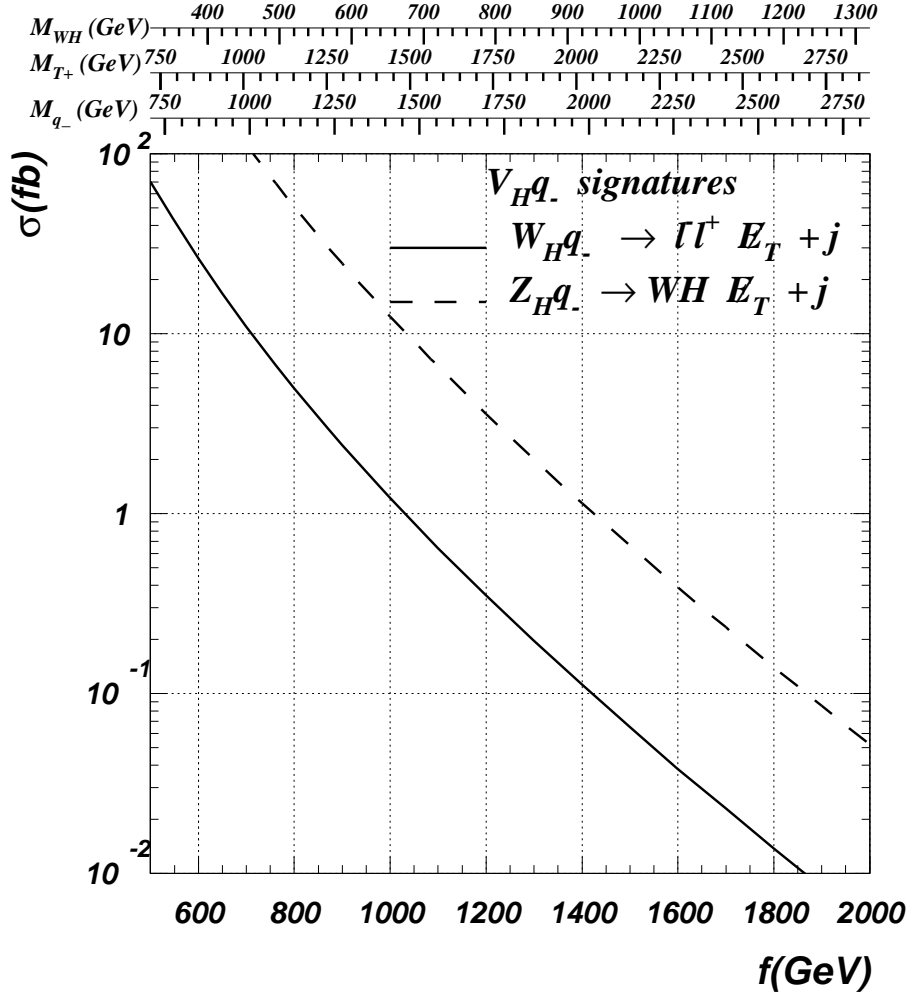


FIG. 15: Rates for opposite-sign lepton and associate Higgs production signatures from T-odd boson and T-odd quark associate production, $V_H q_-$, at the LHC.

3. $q_- V_H$ associate production

As discussed in Ref. [16] Higgs boson production rate via gluon-gluon fusion process is always smaller than that predicted by SM. However, because in most part of the model parameter space, a heavy T-odd Z_H decays almost entirely into a ZH pair, it provides new production channels for the SM-like Higgs boson. The experimental signature of the $q_- V_H$ pair production can be classified as follows.

1) $q_- W_H$ production

This signal process gives rise to OSL and 1L signatures with one less jet as compared to the T-odd heavy quark pair production, but without the LSL signature. The OSL signature

rate for this process is presented as the solid line in Fig. 15.

2) $q_- Z_H$ production

The interesting decay chain of this signal process is $q_- Z_H \rightarrow q' W_H Z_H \rightarrow q' W^+ A_H A_H H$ in which a high P_T Higgs boson is associatively produced with a W -boson. Its event rate is large, at about 12 fb level for $f = 1$ TeV and $\kappa = 1$. With a large \cancel{E}_T in the event, it could be detectable, though a detailed Monte Carlo study is needed. The respective rate for $q' W^+ A_H A_H H$ signature is presented in Fig. 15 by the dashed line.

3) $q_- A_H$ production

The decay chain $q_- A_H \rightarrow W_H q' A_H \rightarrow W A_H q' A_H$ provides the $W^\pm + \cancel{E}_T$ signature which is however not a promising channel to look for the signal, because the SM backgrounds, such as the $WZ(\rightarrow \nu\nu)$ production, could be quite large.

4. $V_H V_H$ production

The experimental signatures of $V_H V_H$ events are similar to that of $q_- V_H$ events, but with one less high- P_T jet. Therefore, it requires a larger production cross section to detect such a signal event.

1) $Z_H W_H$ production

The event rate of $Z_H W_H \rightarrow A_H H W A_H$ is about the same as that for $q_- V_H$ production, but with almost 100% decay branching ratio. The rate as a function of f is presented in Fig. 16 by the dashed line. Its experimental signature is the WH associate production with large missing \cancel{E}_T .

2) $W_H^+ W_H^-$ production

The event rate of $W_H^+ W_H^- \rightarrow W^+ A_H W^- A_H$ is about 5 times smaller than that for $q_- V_H$ production. The solid line of Fig. 16 presents this OSL signature rate. Hence, it is more challenging to detect such a signal event in the pure leptonic channel.

3) $Z_H Z_H$ production

The event signature of $Z_H Z_H \rightarrow A_H H A_H H$ is the production of a pair of Higgs bosons with large \cancel{E}_T in the event. Its production rate is about one order of magnitude smaller than the $W_H^+ W_H^-$ production rate, as indicated by the dot-dashed line in Fig. 16. On the other hand, in spite of its small production rate, this process offers an interesting production channel for Higgs boson pairs.

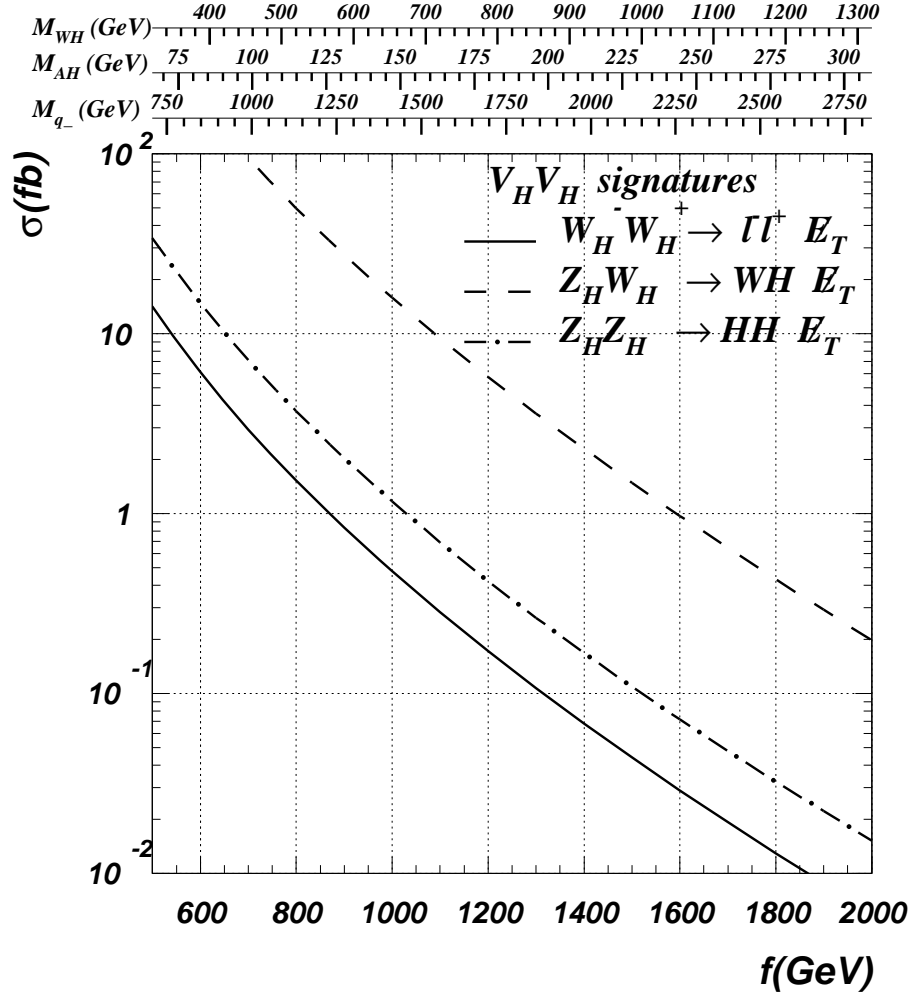


FIG. 16: Rates for OSL, WH and HH signatures for various $V_H V_H$ production reactions at the LHC.

5. Heavy T-odd Higgs boson production

The highest heavy T-odd Higgs production rate, with its cross section around 1 fb for $f \simeq 1$ TeV, comes from the $\phi^{++}\phi^-$ or $\phi^{--}\phi^+$ production channels. For the model parameters under study, there is no allowed two-body decay mode for ϕ^{++} boson, due to mass constraints. Nevertheless, 3-body decay modes of ϕ^{++} can take place at tree level, and it is also possible to have 2-body radiative decay modes dominating the decay branching ratios of ϕ^{++} . Hence, there will be multiple jets and leptons in such kind of signal events.

V. CONCLUSIONS

The Littlest Higgs model with T-parity (LHT) [5, 6, 7, 8] is an attractive Little Higgs model which provides not only solution to the Little hierarchy problem but also a possible dark matter candidate [9]. Because of the T-parity, T-odd gauge bosons contribute to the electroweak observables at the weak scale in pairs, hence, the mass scale (f) of new particles predicted in this model can be as low as 500 GeV [7]. With the possibility of such a low mass scale, many interesting phenomenology has been studied in the literature [6]. In order to implement T-parity in the fermion sector of the model, the heavy T-odd $SU(2)$ -doublet fermions, which are T-parity partners of the SM fermion doublets, have to be introduced. A preliminary study on the phenomenology of these T-odd $SU(2)$ -doublet fermions in the LHT was reported in Ref. [10]. In this paper, we present a detailed study of the phenomenology of the LHT with the emphasis on the role of the T-odd fermions in high energy scattering processes at the LHC.

In Sec. II, we present the effective Lagrangian of the LHT studied in this paper. Some relevant Feynman rules are also summarized in Appendix A. Particular attention has been given to discussing the properties of those T-odd $SU(2)$ -doublet fermions (denoted as q_-), including their masses and interactions to other particles predicted in the model. As shown in Eq. (9), their masses are about $\sqrt{2}\kappa f$ where κ is the coefficient introduced in the interaction Lagrangian, cf. Eq. (8), for generating a large mass to q_- . (For simplicity, we have assumed a constant κ value, independent of quark flavor and family.) While the typical cutoff scale of the effective theory is about $4\pi f$, the mass of the T-odd $SU(2)$ -doublet fermions is bounded from above due to the low energy constraint induced by the four-fermion contact interaction presented in Eq. (10). Hence, in our study the κ value is required to be less than about 3.4 for f about 1 TeV. Similar kind of constraints on the two parameters (λ_1 and λ_2) in the top quark sector are also discussed in Sec. II. The results are given in Eqs. (17), (18) and (20). A detailed discussion on the $J = 1$ partial-wave amplitudes in the coupled system of $(t\bar{t}, T_+\bar{T}_+, b\bar{b}, WW, Zh)$ states, which are relevant to the top Yukawa coupling, is presented in Appendix B. Finally, we note that the T-parity symmetry is correctly implemented in our effective Lagrangian such that the $[SU(2) \times U(1)]^2$ gauge symmetry is non-linearly realized in all sectors, including the bottom quark Yukawa interaction sector. (It differs from the model presented in Ref. [6] in which the similar sector is not gauge invariant.)

In Sec. III, we stress the importance of the T-odd $SU(2)$ doublet fermion contributions to high energy processes. As an example, we discuss the high energy behavior of $u\bar{u} \rightarrow W_H^+ W_H^-$ through partial-wave analysis. To have a gauge-invariant amplitude, both types of Feynman diagrams shown in Fig. 2 need to be included in order to satisfy unitarity condition in high energy collision. Furthermore, as shown in Sec. II, the mass of q_- is bounded from above by low energy data in this effective theory. Therefore, the decoupling limit of the T-odd fermions is not a realistic assumption and the T-odd fermion contribution generates important correction to $u\bar{u} \rightarrow W_H^+ W_H^-$ process, which has not been taken into account in the previous study [6].

Because the mass of the T-odd $SU(2)$ doublet fermions cannot be too heavy, cf. Eq. (10), they can be copiously produced at the LHC. Therefore, in Sec. IV, we study the collider phenomenology of the LHT with emphasis on the contributions of the T-odd fermion to the production of the heavy T-parity partners (either bosons or fermions) at the LHC. Fig. 6 shows the production cross sections of the first and second generation heavy T-odd quarks. As shown, their cross sections are quite sizable at the LHC. In Fig. 7, we show the similar plot for the third generation heavy T-odd and T-even quarks. As discussed in Sec. II, the LHT contains additional T-odd and T-even heavy quarks which are the T-parity partners of top quark. The T-even partner (T_+) of top quark can be produced singly or in pairs. We also show in Fig. 8 the associate production cross section of T-odd fermions and T-odd gauge bosons. The associate production cross sections of T_+ and weak gauge bosons are also shown in the same figure. In Fig. 9, we show the production cross sections of heavy T-odd gauge boson pairs. As an illustration, the dependence of the $pp \rightarrow W_H^+ W_H^-$ production on the mass of T-odd fermion is given in Fig. 10. For completeness, we also show the production rate of heavy T-odd Higgs bosons in Fig. 11, though their production rates are generally small.

Before we discuss the probable experimental signatures predicted by this model at the LHC, we presented typical decay branching channels of the T-parity partners in Table III and Fig. 12. It turns out that the result of Table III is not very sensitive to the choice of model parameters such as f , λ_1 , s_α and M_H for T-odd fermions. Similarly, Fig. 12 also presents a typical pattern of branching ratios for T-even heavy top-quark partner T_+ , though this pattern depends on the choice of model parameters such as s_α and M_H .

Combining the information on the production cross section of heavy particles and their

decay branching ratios into particular decay channels, one can easily calculate production rates of events with certain experimental signature. Some of those results are shown in the remaining figures of the paper.

We concluded in Sec. IV that the like-sign di-lepton signature of the 1st and 2nd generation heavy T-odd quark pair production is the most useful channel to discover these new heavy quarks at the LHC. Because the heavy T-odd gauge boson Z_H almost always decays into a pair of Higgs boson H and T-odd photon A_H , the production processes with Z_H in the final state provide a new production mechanism for single-Higgs or Higgs-pair production. Their rates are presented in Figs. 15 and 16, respectively.

We also provide for the first time the complete CalcHEP LHT model files including T-odd $SU(2)$ doublet fermions, which is available at <http://hep.pa.msu.edu/LHT/>.

Acknowledgments

We thank Qing-Hong Cao, Jay Hubisz, Alexander Pukhov and Riccardo Rattazzi for useful discussions. C.P.Y. and K.T. thank the National Center for Theoretical Sciences in Taiwan for its hospitality, where part of the work was done. This work was supported in part by the US National Science Foundation under award PHY-0555545.

Note added: While finalizing the write-up of this work, we are aware of the paper by A. Freitas and D. Wyler [31] who studied the phenomenology of T-odd fermion in the LHT.

APPENDIX A: FEYNMAN RULES

Most of the Feynman rules for the Littlest Higgs model with T-parity have been presented in Ref. [6] and the references therein except for T-odd $SU(2)$ doublet fermions. We agree with their results in the hep-ph arXiv version (v3) of Ref. [6] after identifying $T_+ = -t'_+$ and $T_- = -t'_-$ (their t'_\pm fields correspond to our T_\pm). In this appendix, we list a few Feynman rules relevant to our analysis, especially those related to T-odd fermions. They are listed in Tables IV–VI below.

We also provide for the first time the complete CalcHEP LHT model files including T-odd $SU(2)$ doublet fermions which is available at <http://hep.pa.msu.edu/LHT/>.

In Tables IV, V and VI, we have defined the following coefficients. $s_H (= \sin \theta_H)$ describes the degree of mixing between heavy neutral gauge bosons with $s_H \simeq \frac{gg'}{g^2 - g'^2/5} \frac{v_{SM}^2}{4f^2}$ and $c_H = \cos \theta_H$. Also, $s_L \simeq s_\alpha^2 \frac{v_{SM}}{f}$ and $c_L = \sqrt{1 - s_L^2}$. In addition, $P_L = \frac{1 - \gamma_5}{2}$ and $P_R = \frac{1 + \gamma_5}{2}$ are the left-handed and right-handed projection operators, respectively. We note that in those tables we have suppressed the CKM matrix element dependence. For example, from Table VI, we can read out the coupling of $W_\mu^+ \bar{t} b$ to be $V_{tb}(i \frac{g}{\sqrt{2}} c_L \gamma_\mu P_L)$, after restoring the CKM matrix element V_{tb} derived from the interaction Lagrangian. In the above expression, the product of $V_{tb} c_L$, which is defined as V_{tb}^{eff} , should be identified with the CKM matrix element determined from the low energy processes (or from measuring the SM single-top direct production rate at the Tevatron or the LHC [27, 28]). Thus, from Table VI, we read out the coupling of $W^+ \bar{T}_+ b$ to be $V_{tb}(i \frac{g}{\sqrt{2}} s_L \gamma_\mu P_L)$, after restoring the CKM matrix element dependence, which can be rewritten as $V_{tb}^{eff}(i \frac{g}{\sqrt{2}} \frac{s_L}{c_L} \gamma_\mu P_L)$. The coefficient of $W^+ \bar{T}_+ b$ coupling $V_{tb}^{eff} \frac{s_L}{c_L}$ is approximately equal to $V_{tb}^{eff} s_L$ up to v_{SM}^2/f^2 corrections, for $s_L \propto v_{SM}/f$, cf. Eq. (15).

Interaction	Feynman rule	Interaction	Feynman rule
$W_{H_\mu}^+ \bar{u} d_-$	$i \frac{g}{\sqrt{2}} \gamma_\mu P_L$	$W_{H_\mu}^- \bar{d} u_-$	$i \frac{g}{\sqrt{2}} \gamma_\mu P_L$
$Z_{H_\mu} \bar{u} u_-$	$i(\frac{gc_H}{2} - \frac{g's_H}{10}) \gamma_\mu P_L$	$Z_{H_\mu} \bar{d} d_-$	$i(-\frac{gc_H}{2} - \frac{g's_H}{10}) \gamma_\mu P_L$
$A_{H_\mu} \bar{u} u_-$	$i(-\frac{gs_H}{2} - \frac{g'c_H}{10}) \gamma_\mu P_L$	$A_{H_\mu} \bar{d} d_-$	$i(\frac{gs_H}{2} - \frac{g'c_H}{10}) \gamma_\mu P_L$

TABLE IV: Feynman rules for the 1st and 2nd generation T-odd fermion interaction with heavy gauge boson and SM fermion.

APPENDIX B: UNITARITY BOUND FROM $J = 1$ PARTIAL WAVE AMPLITUDES IN THE COUPLED SYSTEM OF $(t\bar{t}, T_+ \bar{T}_+, b\bar{b}, WW, Zh)$ STATES

The amplitudes for $t\bar{t} \rightarrow t\bar{t}, T_+ \bar{T}_+, b\bar{b}, WW$, and Zh processes and their inverse processes contribute to $J = 1$ partial wave amplitude matrix in this coupled system. The $J = 1$ partial wave amplitudes are given by

$$a_{\mu\mu'}^1 = \frac{1}{32\pi} \int_{-1}^1 d(\cos \theta) d_{\mu\mu'}^1(\theta) T_{\mu\mu'}. \quad (B1)$$

Here $d_{\mu\mu'}^1(\theta)$ is the well-known Wigner d-function. For fermions, μ and μ' are defined by $\mu = (\lambda - \bar{\lambda})/2$ and $\mu' = (\lambda' - \bar{\lambda}')/2$, where λ 's are the helicities of the fermions: λ ($\bar{\lambda}$) for

Interaction	Feynman rule	Interaction	Feynman rule
$W_{H_\mu}^+ \bar{t}b_-$	$i\frac{g_{cL}}{\sqrt{2}}\gamma_\mu P_L$	$W_{H_\mu}^- \bar{b}t_-$	$i\frac{g}{\sqrt{2}}\gamma_\mu P_L$
$W_{H_\mu}^+ \bar{T}_+ b_-$	$i\frac{g_{sL}}{\sqrt{2}}\gamma_\mu P_L$		
$Z_{H_\mu} \bar{t}t_-$	$i(\frac{g_{cH}}{2} - \frac{g'_{sH}}{10})c_L\gamma_\mu P_L$	$Z_{H_\mu} \bar{b}b_-$	$i(-\frac{g_{cH}}{2} - \frac{g'_{sH}}{10})\gamma_\mu P_L$
$Z_{H_\mu} \bar{T}_+ t_-$	$i(\frac{g_{cH}}{2} - \frac{g'_{sH}}{10})s_L\gamma_\mu P_L$	$Z_{H_\mu} \bar{t}T_-$	$-i\frac{2}{5}g's_H\gamma_\mu(s_L P_L + s_R P_R)$
$Z_{H_\mu} \bar{T}_+ T_-$	$i\frac{2}{5}g's_H\gamma_\mu(c_L P_L + c_R P_R)$		
$A_{H_\mu} \bar{t}t_-$	$i(-\frac{g_{sH}}{2} - \frac{g'_{cH}}{10})c_L\gamma_\mu P_L$	$A_{H_\mu} \bar{b}b_-$	$i(\frac{g_{sH}}{2} - \frac{g'_{cH}}{10})\gamma_\mu P_L$
$A_{H_\mu} \bar{T}_+ t_-$	$i(-\frac{g_{sH}}{2} - \frac{g'_{cH}}{10})s_L\gamma_\mu P_L$	$A_{H_\mu} \bar{t}T_-$	$-i\frac{2}{5}g'c_H\gamma_\mu(s_L P_L + s_R P_R)$
$A_{H_\mu} \bar{T}_+ T_-$	$i\frac{2}{5}g'c_H\gamma_\mu(c_L P_L + c_R P_R)$		

TABLE V: Feynman rules for the 3rd generation T-odd fermion interaction with heavy gauge boson and SM fermion.

Interaction	Feynman rule	Interaction	Feynman rule
$W_\mu^+ \bar{t}b$	$i\frac{g}{\sqrt{2}}c_L\gamma_\mu P_L$	$W^+ \bar{T}_+ b$	$i\frac{g}{\sqrt{2}}s_L\gamma_\mu P_L$
$Z_\mu \bar{t}t$	$i\frac{g}{c_W}\gamma_\mu \{(\frac{1}{2}c_L^2 - \frac{2}{3}s_W^2)P_L - \frac{2}{3}s_W^2 P_R\}$	$Z_\mu \bar{t}T_+$	$i\frac{g}{c_W}\frac{s_L c_L}{2}\gamma_\mu P_L$
$Z_\mu \bar{T}_+ T_+$	$i\frac{g}{c_W}\gamma_\mu \{(\frac{1}{2}s_L^2 - \frac{2}{3}s_W^2)P_L - \frac{2}{3}s_W^2 P_R\}$		

TABLE VI: Feynman rules for the SM gauge interaction with top sector.

the initial state fermion (anti-fermion) and λ' ($\bar{\lambda}'$) for the final state fermion (anti-fermion), and for bosons, $\mu = 0$. $T_{\mu\mu'}$ is a helicity amplitude with μ and μ' .

Writing the channels in the order $t_+ \bar{t}_-$, $(T_+)_+(T_+)_-$, $W^+ W^-$, hZ , $t_- \bar{t}_+$ and $b_- \bar{b}_+$, the $J = 1$ partial wave amplitude matrix a^1 is given by

$$a^1 = \frac{M_t^2}{16\pi v_{SM}} \begin{pmatrix} 0 & 0 & -\sqrt{2} & -i\sqrt{2} & -1 & +1 \\ 0 & 0 & -\sqrt{2}R^2 & -i\sqrt{2}R^2 & R^2 & R^2 \\ -\sqrt{2} & -\sqrt{2}R^2 & 0 & 0 & 0 & \sqrt{2}(1+R^2) \\ i\sqrt{2} & i\sqrt{2}R^2 & 0 & 0 & i\sqrt{2}(1+R^2) & 0 \\ -1 & R^2 & 0 & -i\sqrt{2}(1+R^2) & 0 & 0 \\ 1 & R^2 & \sqrt{2}(1+R^2) & 0 & 0 & 0 \end{pmatrix}, \quad (\text{B2})$$

where $R = \lambda_1/\lambda_2$. Here we have assumed that the center-of-mass energy \sqrt{s} is much larger than masses of particles considered here, and only couplings in top sector are relevant, and gauge couplings and all other Yukawa couplings are taken to be zero. We have not shown explicitly the color indices in Eq. (B2), however all color neutral channels should be taken into account. Thus the $J = 1$ partial wave amplitude matrix in this system is 14×14 . Note that the parameter R is the only unknown parameter in Eq. (B2), and the absolute value

of the largest eigenvalue of the $J = 1$ partial wave amplitude matrix increases as R gets larger. The requirement that the absolute value of the largest eigenvalue be less than a half ($|a_{\max}^1| < 1/2$) yields the upper bound on the parameter R as

$$R < 3.3, \quad (\text{B3})$$

for $M_t = 175$ GeV. In terms of s_α , this bound corresponds to

$$s_\alpha < 0.96, \quad (\text{B4})$$

since $R = s_\alpha/c_\alpha$. Using the top-quark mass constraint, cf. Eq. (17), this bound generates a bound on λ_1 as

$$\lambda_1 = \frac{M_t}{v_{SM}\sqrt{1-s_\alpha^2}} < 2.5, \quad (\text{B5})$$

for $M_t = 175$ GeV.

-
- [1] R. Barbieri and A. Strumia, arXiv:hep-ph/0007265.
 - [2] N. Arkani-Hamed, A. G. Cohen and H. Georgi, “Electroweak symmetry breaking from dimensional deconstruction,” *Phys. Lett. B* **513**, 232 (2001) [arXiv:hep-ph/0105239]. For reviews, see, for example, M. Schmaltz and D. Tucker-Smith, “Little Higgs review,” arXiv:hep-ph/0502182; M. Perelstein, “Little Higgs models and their phenomenology,” arXiv:hep-ph/0512128; and references therein.
 - [3] N. Arkani-Hamed, A. G. Cohen, E. Katz and A. E. Nelson, “The Littlest Higgs,” *JHEP* **0207**, 034 (2002) [arXiv:hep-ph/0206021].
 - [4] C. Csaki, J. Hubisz, G. D. Kribs, P. Meade and J. Terning, “Big corrections from a little Higgs,” *Phys. Rev. D* **67**, 115002 (2003) [arXiv:hep-ph/0211124]. J. L. Hewett, F. J. Petriello and T. G. Rizzo, “Constraining the littlest Higgs,” *JHEP* **0310**, 062 (2003) [arXiv:hep-ph/0211218]. C. Csaki, J. Hubisz, G. D. Kribs, P. Meade and J. Terning, “Variations of little Higgs models and their electroweak constraints,” *Phys. Rev. D* **68**, 035009 (2003) [arXiv:hep-ph/0303236]. M. C. Chen and S. Dawson, “One-loop radiative corrections to the rho parameter in the littlest Higgs model,” *Phys. Rev. D* **70**, 015003 (2004) [arXiv:hep-ph/0311032]. W. Kilian and J. Reuter, *Phys. Rev. D* **70**, 015004 (2004) [arXiv:hep-ph/0311095]. Z. Han and W. Skiba, “Effective theory analysis of precision electroweak data,” *Phys. Rev. D* **71**, 075009 (2005) [arXiv:hep-ph/0412166].
 - [5] I. Low, “T parity and the littlest Higgs,” *JHEP* **0410**, 067 (2004) [arXiv:hep-ph/0409025].
 - [6] J. Hubisz and P. Meade, “Phenomenology of the littlest Higgs with T-parity,” *Phys. Rev. D* **71**, 035016 (2005) [arXiv:hep-ph/0411264].
 - [7] J. Hubisz, P. Meade, A. Noble and M. Perelstein, “Electroweak precision constraints on the littlest Higgs model with T JHEP **0601**, 135 (2006) [arXiv:hep-ph/0506042].
 - [8] H. C. Cheng and I. Low, “TeV symmetry and the Little hierarchy problem,” *JHEP* **0309**, 051 (2003) [arXiv:hep-ph/0308199]; “Little hierarchy, Little Higgses, and a Little symmetry,” *JHEP* **0408**, 061 (2004) [arXiv:hep-ph/0405243].
 - [9] M. Asano, S. Matsumoto, N. Okada and Y. Okada, “Cosmic positron signature from dark matter in the littlest Higgs model with T-parity,” arXiv:hep-ph/0602157. A. Birkedal, A. Noble, M. Perelstein and A. Spray, “Little Higgs dark matter,” *Phys. Rev. D* **74**, 035002 (2006) [arXiv:hep-ph/0603077].

- [10] A. Belyaev, C.-R. Chen, K. Tobe and C.-P. Yuan, Talk at Monte Carlo Tools for Beyond the Standard Model Physics (March 2006, Fermilab) given by A. Belyaev, <http://theory.fnal.gov/mc4bsm/agenda.html>; talk at Osaka university (May 2006, Osaka) given by C.-P. Yuan, <http://www-het.phys.sci.osaka-u.ac.jp/seminar/seminar/seminar.html>; talk at 2006 Summer Institute on Collider Phenomenology (June 2006, National Tsing Hua University, Taiwan) given by K. Tobe, <http://charm.phys.nthu.edu.tw/~hep/summer2006/> and talk at ICHEP'06 (July 2006, Moscow) given by A. Belyaev, http://ichep06.jinr.ru/reports/116_11s1_10p20_belyaev.pdf
- [11] C. S. Chen, K. Cheung and T. C. Yuan, "Novel collider signature for little Higgs dark matter models," arXiv:hep-ph/0605314.
- [12] T. Han, H. E. Logan, B. McElrath and L. T. Wang, "Phenomenology of the little Higgs model," Phys. Rev. D **67**, 095004 (2003) [arXiv:hep-ph/0301040].
- [13] J. Hubisz, S. J. Lee and G. Paz, "The flavor of a little Higgs with T-parity," arXiv:hep-ph/0512169; M. Blanke, A. J. Buras, A. Poschenrieder, C. Tarantino, S. Uhlig and A. Weiler, "Particle antiparticle mixing, ϵ_K , $\Delta\Gamma_q$, A_{SL}^q , $A_{CP}(B/d \rightarrow \psi K_S)$, $A_{CP}(B_s \rightarrow \psi\phi)$ and $B \rightarrow X_{s,d}\gamma$ in the lightest Higgs model with T-parity," arXiv:hep-ph/0605214.
- [14] M. S. Chanowitz, M. A. Furman and I. Hinchliffe, "Weak Interactions Of Ultraheavy Fermions," Phys. Lett. B **78**, 285 (1978); "Weak Interactions Of Ultraheavy Fermions. 2," Nucl. Phys. B **153**, 402 (1979).
- [15] J. Hubisz, unpublished work.
- [16] C. R. Chen, K. Tobe and C.-P. Yuan, "Higgs boson production and decay in little Higgs models with T-parity," arXiv:hep-ph/0602211.
- [17] J. L. Hewett, F. J. Petriello and T. G. Rizzo, "Constraining the lightest Higgs. ((U))," JHEP **0310**, 062 (2003) [arXiv:hep-ph/0211218].
- [18] G. Burdman, M. Perelstein and A. Pierce, "Collider tests of the little Higgs model," Phys. Rev. Lett. **90**, 241802 (2003) [Erratum-ibid. **92**, 049903 (2004)] [arXiv:hep-ph/0212228].
- [19] M. Perelstein, M. E. Peskin and A. Pierce, "Top quarks and electroweak symmetry breaking in little Higgs models," Phys. Rev. D **69**, 075002 (2004) [arXiv:hep-ph/0310039].
- [20] T. Han, H. E. Logan and L. T. Wang, "Smoking-gun signatures of little Higgs models," JHEP **0601**, 099 (2006) [arXiv:hep-ph/0506313].
- [21] H. C. Cheng, I. Low and L. T. Wang, "Top partners in little Higgs theories with T-parity," arXiv:hep-ph/0510225.
- [22] C. F. Berger, M. Perelstein and F. Petriello, "Top quark properties in little Higgs models," arXiv:hep-ph/0512053.
- [23] P. Meade and M. Reece, "Top partners at the LHC: Spin and mass measurement," Phys. Rev. D **74**, 015010 (2006) [arXiv:hep-ph/0601124].
- [24] J. Pumplin, D. R. Stump, J. Huston, H. L. Lai, P. Nadolsky and W. K. Tung, "New generation of parton distributions with uncertainties from global QCD JHEP **0207**, 012 (2002) [arXiv:hep-ph/0201195].
- [25] A. Pukhov, "CalcHEP 3.2: MSSM, structure functions, event generation, batches, and arXiv:hep-ph/0412191.
- [26] A. Semenov, "LanHEP: A package for automatic generation of Feynman rules from the Comput. Phys. Commun. **115** (1998) 124.
- [27] C.-P. Yuan, Phys. Rev. D **41**, 42 (1990).
- [28] S. Dawson, "The Effective W Approximation," Nucl. Phys. B **249**, 42 (1985); S. S. D. Willenbrock and D. A. Dicus, "Production Of Heavy Quarks From W Gluon Fusion," Phys. Rev. D **34**, 155 (1986); R. K. Ellis and S. J. Parke, "Top quark production by W gluon fusion," Phys. Rev. D **46**, 3785 (1992); D. O. Carlson and C.-P. Yuan, "Studying the top quark via the W - gluon fusion process," Phys. Lett. B **306**, 386 (1993); G. Bordes and B. van Eijk, "Calculating QCD corrections to single top production in hadronic Nucl. Phys. B **435**, 23 (1995); A. P. Heinson, A. S. Belyaev and E. E. Boos, "Single top quarks at the Fermilab Tevatron," Phys. Rev. D **56**, 3114 (1997) [arXiv:hep-ph/9612424]; T. Stelzer, Z. Sullivan and S. Willenbrock, "Single-top-quark production via W-gluon fusion at next-to-leading order," Phys. Rev. D **56**, 5919 (1997) [arXiv:hep-ph/9705398]; Q. H. Cao, R. Schwienhorst, J. A. Benitez, R. Brock and C.-P. Yuan, "Next-to-leading order corrections to single top quark production and decay at the Tevatron. II: t-channel process," Phys. Rev. D **72**, 094027 (2005) [arXiv:hep-ph/0504230].

- [29] J. Bagger *et al.*, “The Strongly interacting W W system: Gold plated modes,” Phys. Rev. D **49**, 1246 (1994) [arXiv:hep-ph/9306256]; J. Bagger *et al.*, “LHC analysis of the strongly interacting W W system: Gold plated modes,” Phys. Rev. D **52**, 3878 (1995) [arXiv:hep-ph/9504426].
- [30] S. Abachi *et al.* [D0 Collaboration], Phys. Rev. Lett. **74**, 2632 (1995) [arXiv:hep-ex/9503003]; F. Abe *et al.* [CDF Collaboration], Phys. Rev. Lett. **74**, 2626 (1995) [arXiv:hep-ex/9503002].
- [31] A. Freitas and D. Wyler, “Phenomenology of mirror fermions in the littlest Higgs model with T-parity,” arXiv:hep-ph/0609103.